

Perspective

Immobilization of Polyoxometalates on Carbon Nanotubes: Tuning Catalyst Activity, Selectivity and Stability in H₂O₂-Based Oxidations

Vasilii Yu. Evtushok ^{1,2}, Vladimir A. Lopatkin ^{1,2} , Olga Yu. Podyacheva ¹  and Oxana A. Kholdeeva ^{1,*}

¹ Boreskov Institute of Catalysis, Lavrentieva Ave. 5, 630090 Novosibirsk, Russia; evtvas@catalysis.ru (V.Y.E.); v.lopatkin@ng.su.ru (V.A.L.); pod@catalysis.ru (O.Y.P.)

² Novosibirsk State University, Pirogova Str. 2, 630090 Novosibirsk, Russia

* Correspondence: khold@catalysis.ru

Abstract: In recent years, carbon nanotubes (CNTs), including N-doped ones (N-CNTs), have received significant attention as supports for the construction of heterogeneous catalysts. In this work, we summarize our progress in the application of (N)-CNTs for immobilization of anionic metal-oxygen clusters or polyoxometalates (POMs) and use of (N)-CNTs-supported POM as catalysts for liquid-phase selective oxidation of organic compounds with the green oxidant—aqueous hydrogen peroxide. We discuss here the main factors, which favor adsorption of POMs on (N)-CNTs and ensure a quasi-molecular dispersion of POM on the surface and their strong attachment to the support. The effects of the POM nature, N-doping of CNTs, acid additives, and other factors on the POM immobilization process and catalytic activity/selectivity of the (N)-CNTs-immobilized POMs are analyzed. Particular attention is drawn to the critical issue of the catalyst stability and reusability. The scope and limitations of the POM/(N)-CNTs catalysts in H₂O₂-based selective oxidations are discussed.

Keywords: heterogeneous catalysis; hydrogen peroxide; liquid-phase selective oxidation; polyoxometalates; carbon nanotubes; N-doping; supported catalysts



Citation: Evtushok, V.Y.; Lopatkin, V.A.; Podyacheva, O.Y.; Kholdeeva, O.A. Immobilization of Polyoxometalates on Carbon Nanotubes: Tuning Catalyst Activity, Selectivity and Stability in H₂O₂-Based Oxidations. *Catalysts* **2022**, *12*, 472. <https://doi.org/10.3390/catal12050472>

Academic Editor: Sabine Valange

Received: 23 March 2022

Accepted: 20 April 2022

Published: 22 April 2022

Publisher's Note: MDPI stays neutral with regard to jurisdictional claims in published maps and institutional affiliations.



Copyright: © 2022 by the authors. Licensee MDPI, Basel, Switzerland. This article is an open access article distributed under the terms and conditions of the Creative Commons Attribution (CC BY) license (<https://creativecommons.org/licenses/by/4.0/>).

1. Introduction

The selective oxidation of organic compounds is an indispensable methodology for the synthesis of many oxygen-containing intermediates and valuable products of modern organic synthesis [1,2]. While thermally stable compounds, such as ethylene oxide, formaldehyde, phthalic anhydride and others, are produced industrially by gas-phase catalytic oxidation, less stable base chemicals (more than half of the selective oxidation products) are obtained in liquid-phase processes. Moreover, liquid-phase oxidation is the predominant way for the synthesis of many fine chemicals, which cannot survive under harsh conditions of gas-phase oxidation. One of the most promising approaches in the selective oxidation is considered to be the use of heterogeneous catalysts and green oxidizing agents, such as molecular oxygen and hydrogen peroxide [3–5]. Aqueous hydrogen peroxide is a relatively cheap industrially manufactured product and atom-efficient reagent, which yields water and molecular oxygen as the sole byproducts [6,7]. Despite modern progress in designing principles of heterogeneous selective oxidation catalysts that would be tolerant to leaching in the liquid phase, the development of such catalysts remains a difficult task and leaves room for research work.

Polyoxometalates (POM) are early-transition metal anionic metal-oxygen clusters [8–11]. They are usually divided into two main groups, isopolyanions containing only one type of metal ions, and heteropolyanions that also comprised of heteroatoms, which can include different metal ions or nonmetals (P, Si, As, etc.). Both groups can be represented by the general formulas [M_xO_y]^{q-} for isopolyanions and [X_nM_xO_y]^{q-} (n ≤ x) for heteropolyanions, where M is the structural transition metal (also called addendum) and X is heteroatom.

Addenda metals are usually Mo, W, V, Nb, and Ta in their highest oxidation states; however, a part of them can be substituted for other transition metals. There is a wide variety of POM structures, which are usually built from octahedrally coordinated metal atoms and have high symmetry. POMs are being intensively studied in various fields of catalysis [12–18] and materials science [19–22]. The increased interest in POMs is promoted by their tunable acid-base and redox properties, thermal and hydrolytic stability. Many POM-based catalytic systems that employ hydrogen peroxide as an oxidant have been developed for liquid-phase selective oxidations [13,17,23–27]. Similar to d-metal complexes with organic ligands, some POMs are capable of activating hydrogen peroxide via a heterolytic mechanism, that is, without the formation of radicals. This feature means high selectivity can be achieved in various oxidation reactions catalyzed by POMs. Moreover, in contrast to conventional metal complexes, POMs possess an inorganic nature and endow thermodynamic stability to oxidation.

High efficiency of POMs in homogeneous selective oxidation of organic compounds with H_2O_2 has stimulated numerous attempts to design heterogeneous catalysts by immobilization of POMs on various supports [28–32]. A major part of reported POM immobilizations for catalytic oxidation relies on electrostatic interaction with supports such as surface-modified silicas [33–43], metal oxides [44–48], hydrotalcites [49–51], ion-exchange polymers [52–55], carbon materials [56–58] and metal-organic frameworks [59–61]. Other approaches, such as immobilization within supramolecular assemblies [62–66], non-covalent binding [67–69], embedding in support pores [70–73], and covalent attachment [74–76], are also employed. However, activity of immobilized POMs is often lower than that of parent homogeneous POMs [37,44,52,54]. In addition, since H_2O_2 is a fairly polar compound and has perhydrolyzing ability, a typical problem with heterogeneous POM catalysts is the leaching of active metals into the reaction mixture [43,46,49,62]. Severe leaching can lead to a loss of activity after catalyst recycling due to a lowering of the content of active POM. However, even small leaching in the range of 10–50 ppm can contaminate the organic product with transition metals, resulting in the need for additional purification steps.

Carbon nanomaterials as catalyst supports attract stable interest for many years due to their resistance to relatively aggressive media (mild oxidants, acids and bases), high surface area, electric conductivity and possibility to control surface properties [77]. Materials based on POMs and carbon nanotubes (CNTs) have drawn significant attention in electrocatalysis [78–80] and energy storage applications [81–89]. However, oxidation catalysis was practically not touched upon in the POM/CNTs studies [90–93]. Presently, methods of POM/CNTs immobilization employ electrostatic attachment [78,79,87,93], π - π interaction [89], and covalent binding [83,84]. In rare cases, immobilization was achieved on pristine CNTs by adsorption during ultrasonication [80,86,94], precipitation [85] or impregnation [91,92]. The chemical inertness of CNTs often requires preliminary functionalization via oxidation or coating with binders.

It is known that the use of nitrogen-doped carbon nanomaterials gives additional scenarios to change the dispersion and electronic state of the supported active component. Impressive results of the use of N-doped carbons were documented for the synthesis of supported metal catalysts as single atoms, showing increased activity in hydrogenation, hydrogen production, oxidation, and other chemical transformations [95]. Thus, nitrogen-doped carbon nanotubes (N-CNTs) can be considered a viable alternative to CNTs due to their built-in nitrogen functional groups and higher tendency to interact with catalytically active particles and molecules [96–99].

In recent years, our group carried out studies on the adsorption of various POMs on (N)-CNTs and investigated catalytic properties of the elaborated POM/(N)-CNTs materials in liquid-phase selective oxidation processes with aqueous hydrogen peroxide as an oxidant [100–103]. The results of the catalytic studies on POM/(N)-CNTs have shown that they are promising heterogeneous catalysts for practical use in the preparation of valuable intermediates and products of fine organic synthesis. In this work, we analyze the previously obtained results and demonstrate how activity, selectivity and stability of

the (N)-CNTs-supported POM catalysts can be tuned for the specific oxidation reaction by the careful choice of the support (CNTs vs N-CNTs, N content), POM nature and loading, solvent, as well as the use of additives.

2. Results and Discussion

2.1. Carbon Support Characterization and POM Adsorption

2.1.1. Carbon Nanotubes Synthesis and Characterization

Multi-walled nitrogen-doped (N-CNTs) and nitrogen-free carbon nanotubes (CNTs) can be synthesized by decomposition of an ethylene-ammonia mixture and ethylene, respectively, on a metal catalyst, Fe-Ni-Al₂O₃, at 700 °C [100–104]. Crude carbon nanotubes are purified by washing with HCl solution until complete leaching of the unencapsulated catalyst. During the synthesis of N-CNTs nitrogen can either be incorporated into the graphene structure with the formation of different N-groups, or simply be captured in the cavities of the nanotubes in the form of N₂. The existence of several types of N-groups in the N-CNTs structure, namely, graphitic (N_Q), pyridinic (N_{Py}), pyrrolic (N_{Pyrr}), and oxide (N_{Ox}) (Figure 1), has been revealed by means of XPS [96,97].

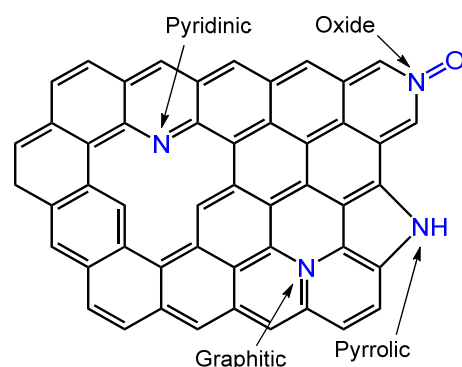


Figure 1. Representation of various nitrogen forms in N-CNTs.

An increase in the concentration of ammonia in the synthesis mixture from 10 to 60 vol. % is accompanied by an increase in the nitrogen content in N-CNTs from 0.8 to 4.8 at. % (Table 1). N-CNTs have a bamboo-like structure and are composed of a series of closed compartments. Enlarging nitrogen content in the structure of N-CNTs leads to an increase in the number of defects [97] and a decrease in the length of the compartments [103]. The correlation between nitrogen content and defect concentration was demonstrated by Raman spectroscopy [97]. At the end of each segment, the open edges of the graphene planes come out to the surface, and thus form regular defects on the surface. The concentration of functional groups and structural defects are important factors for successful POM adsorption; these issues will be discussed below.

Table 1. Total nitrogen content in N-CNTs and the content of different N-groups.

NH ₃ , vol. %	N _{total} , at. %	N _{Py} , %	N _{Pyrr} , %	N _Q , %	N _{Ox} , %	N ₂ , %
10	0.8	23	10	40	10	17
25	1.8	16	13	33	11	27
40	3.1	18	10	32	13	27
60	4.8	27	18	25	10	20

Considering the textural characteristics of carbon nanotubes, we can say that N-CNTs and CNTs are mesoporous materials with a bimodal pore size distribution. Pores with the size of 3–4 nm are formed due to the curvature of graphene layers, whereas larger pores emerge due to the entangled weave of (N)-CNTs leading to the formation of multiple voids.

For (N)-CNTs, the specific surface area and pore volume are normally 150–200 m²/g and 0.5–0.9 cm³/g, respectively [100–102].

2.1.2. POM Adsorption Study

In our studies, POMs were used mostly in the form of tetrabutylammonium (TBA) and tetrahexylammonium (THA) salts due to their high solubility in organic solvents. Usually, POM adsorption on (N)-CNTs was carried out from a solution of POM in acetonitrile and monitored by UV-vis. The adsorption rate was found to be high, and the process takes typically 10–20 min. Successful adsorption on (N)-CNTs was demonstrated for POMs of various structural type, including Keggin H₃PW₁₂O₄₀ (PW₁₂) and TBA₄[γ -HPV₂W₁₀O₄₀] (PV₂W₁₀), Lindqvist TBA_n[NbW₅(L)O₁₈] (NbW₅, where L = O, O-O, OCH₃; n = 3 or 2) and TBA₄[(NbW₅O₁₈)₂O] ((NbW₅)₂O), and Venturello THA₃[PO₄{WO(O₂)₂}]₄ (PW₄). The liquid-phase adsorption has been studied in detail for PV₂W₁₀ [100,102], NbW₅ [103] and PW₄ [101] (structures of these representative POMs are shown in Figure 2).

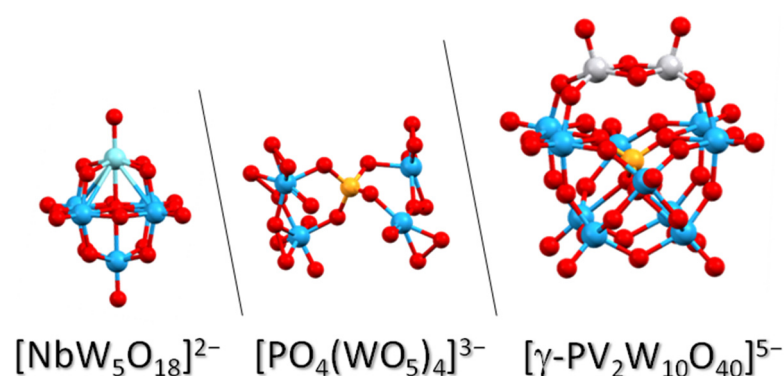


Figure 2. Structures of Lindqvist NbW₅, Venturello PW₄ and Keggin γ -PV₂W₁₀ polyoxometalates.

The most relevant factors that strongly affect POM adsorption on both N-doped and N-free CNTs and do not depend on the specific POM structure are the addition of acid and preliminary drying of the support. Characteristic adsorption isotherms are presented in Figure 3 using PV₂W₁₀ as an example. The addition of acid is crucial, not only for the total amount of adsorption, but also for achieving the irreversible adsorption of POM. The specific relationship between the amount of added HClO₄ and POM adsorption values will be discussed below. Since wetness of (N)-CNTs negatively affects the POM adsorption process, the supports must be dried in a vacuum before their use.

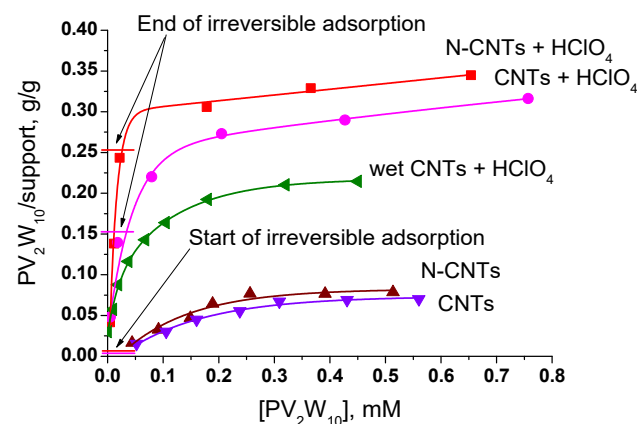


Figure 3. Adsorption of γ -PV₂W₁₀ on CNTs and N-CNTs (4.8 at. % N) from CH₃CN at 25 °C (HClO₄ additives, one equiv to POM). Adapted with permission from ref. [100] Evtushok et al. Highly efficient catalysts based on divanadium-substituted polyoxometalate and N-doped carbon nanotubes for selective oxidation of alkylphenols *ACS Catalysis* 2018, 8, 1297–1307. Copyright 2018 American Chemical Society.

However, acid additives are not necessary if we employ POM in the form of a heteropolyacid. Thus, irreversible adsorption on N-CNTs without help of HClO₄ could be observed for H₃PW₁₂O₄₀ [105]. A sample with 15 wt. % PW₁₂ was obtained under continuous stirring of H₃PW₁₂O₄₀ and N-CNT (1.8 at. % N) in CH₃CN for 24 h. The low adsorption rate might be explained by the low solubility of PW₁₂ in CH₃CN.

Specific values of the maximum (total) and irreversible POM adsorption from CH₃CN on (N)-CNTs are summarized in Table 2. No particular regularity could be found in the amount of adsorbed POM from its charge or size (the size of the POMs studied is within 0.8–1.1 nm range). The values of the irreversible adsorption in the presence of HClO₄ on N-free nanotubes vary from 47 μmol/g for PV₂W₁₀ to 111 μmol/g for NbW₅. Similar values in the range of 50–147 μmol/g were achieved for N-CNTs, although, in general, the irreversible adsorption values were higher for N-CNTs. The amount of HClO₄ added strongly affects the amount of irreversibly adsorbed POM. Increased quantity of acid (2 equiv) allows greater values of irreversible adsorption of NbW₅ and PW₄ to be achieved, while the adsorption of PV₂W₁₀ is not affected (Table 2). A further increase in the HClO₄ quantity (up to 3 equiv) does not lead to a further increase in the amount of irreversibly adsorbed POM, regardless of its structure. Other mineral acids, such as HCl and H₂SO₄, can also be used as additives, but with less effectiveness. Successful adsorption requires larger amounts (5–6 equiv) of these acids.

Table 2. Specific values of irreversible and maximum POM adsorption on CNTs and N-CNTs (1.8 at. % N) from CH₃CN at room temperature.

POM HClO ₄ Additive, equiv.	[PV ₂ W ₁₀ O ₄₀] ⁵⁻			[HNbW ₅ (O ₂)O ₁₈] ²⁻			[PO ₄ {WO(O ₂) ₂] ₄] ³⁻		
	0	1	2	0	1	2	0	1	2
Irreversible Adsorption on CNTs, wt. % (μmol/g)	0	17 (47)	17 (47)	0 (0)	8 (44)	20 (111)	0 (0)	0 (0)	15 (67)
Maximum Adsorption on CNTs, wt. % (μmol/g)	6 (17)	31 (86)	31 (86)	10 (50)	24 (133)	25 (138)	5 (22)	5 (22)	22 (98)
Irreversible Adsorption on N-CNTs, wt. % (μmol/g)	0 (0)	20 (55)	25 (69)	0 (0)	9 (50)	23 (127)	0 (0)	15 (67)	33 (147)
Maximum Adsorption on N-CNTs, wt. % (μmol/g)	8 (22)	28 (77)	36 (100)	10 (55)	24 (133)	28 (155)	15 (67)	22 (98)	37 (165)

Studies by XPS corroborated that the POM adsorption on (N)-CNTs proceeds via an anion exchange mechanism [102] (Figure 4). The signal of adsorbed ClO₄⁻ anions can be clearly distinguished in the XPS spectra of CNTs and N-CNTs treated in HClO₄, thus confirming that HClO₄ acid adsorbs on and protonates the carbon surface. On the other hand, the absence of the ClO₄⁻ signal in the XPS spectrum of PV₂W₁₀/(N)-CNTs indicates that adsorbed ClO₄⁻ ions are exchanged for POM anions during the process of POM immobilization. The protonation of single- and multi-walled CNTs was reported earlier [106–108]. In undoped CNTs, presumably, both O-containing groups (for example, phenolic OH) and carbon in the tube wall with an increased charge density might be protonated. Indeed, the predomination of phenolic groups on the surface of CNTs was recently established by XPS [109]. Note that the protonation of phenols may involve protonation of both the aromatic ring and the hydroxyl group [110,111]. In turn, the protonation of N-CNTs was also documented [112] and supported by DFT calculations, showing that the bonding of proton with pyridinic nitrogen is by ~3.26 eV more preferable than with graphitic N. Presumably, it is the protonated pyridine-like N_{py} that can act as ion-exchange groups.

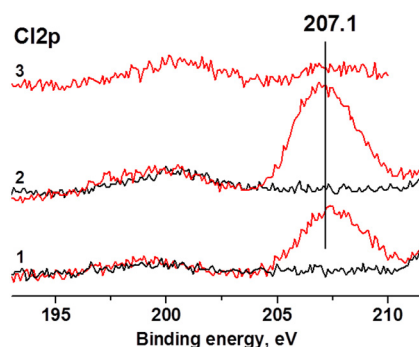


Figure 4. The Cl₂p XPS spectra of CNTs (1), N-CNTs (2), and PV₂W₁₀/N-CNTs (3): initial carbon materials—black curves, treated by HClO₄ (0.15 M in CH₃CN)—red curves). Reprinted from *Catalysis Today*, Vol. 354, Evtushok et al., H₂O₂-based selective oxidations by divanadium-substituted polyoxotungstate supported on nitrogen-doped carbon nanomaterials, 196–203, Copyright 2020, with permission from Elsevier.

The irreversible adsorption of POM is seemingly not limited by the number of O-containing groups in CNTs or N-groups in N-CNTs. According to the XPS data, there is ca. one at. % O in CNTs, which corresponds to 830 μmol/g of O. This is significantly higher than the number of typical values of POM adsorption on CNTs, even taking into account the fact that one ion-exchange group is required for each charge unit of POM. By analogy, for N-CNTs with the nitrogen content of 1.8 at. %, calculation gives 1500 μmol/g of N-groups. If we consider only N_{Py} and N_Q (50% of the total N), then 750 μmol/g N-groups are obtained. This is also significantly higher than the amount of N required to achieve typical POM adsorption values on N-CNTs (see Table 2).

2.1.3. POM/(N)-CNTs Catalysts Characterization

The examination of POM/(N)-CNTs solids using methods of high resolution electron microscopy showed that a nearly quasi-molecular dispersion of PW₄ and PV₂W₁₀ on the surface can be achieved [100,101,103] (Figure 5). While the nitrogen-doping of carbon nanotubes significantly improves PV₂W₁₀ dispersion, the effect seems to be the opposite for PW₄ [101]. The latter fact might be rationalized if we remember that the Venturello complex may form coordinative bonds with N-containing ligands [113], which in turn, may favor the aggregation of PW₄ on the surface. Interestingly, the penetration of POM species into the cavities of some segments of CNTs was observed in the case of PW₄/CNTs [101].

Investigation of NbW₅/(N)-CNTs catalysts morphology and dispersion of POM on the carbon surface by electron microscopy techniques revealed the critical role of defects in the adsorption of NbW₅ [103] (Figure 6). A slight degree of aggregation was observed for catalyst 8 wt. % NbW₅/CNTs (Figure 6c,d). The agglomerates are located on extended defects of CNTs surface and in the cavities between nanotubes. Meanwhile, images of 8 wt. % NbW₅/N-CNTs 4.8 at. % N have shown that nitrogen doping ensures quasi-molecular dispersion of NbW₅ on N-CNTs (Figure 6a,b). The dispersion, apparently, is strongly related to the homogeneity of defect distribution in the nanotubes, and since defects are more evenly distributed in N-CNTs, a higher dispersion of POM is observed. It is very likely that defects also play an important role in the irreversible adsorption of other POMs. However, since NbW₅ has high cohesion (which manifests itself in a tendency to form aggregates [103]), a high density and uniformity of defects is necessary to realize its quasi-molecular dispersion on the surface. The maximum value of NbW₅ adsorption without significant aggregation is 44 μmol/g (corresponds to 8 wt. %), which is quite close to the values of irreversible adsorption acquired for PW₄ and PV₂W₁₀.

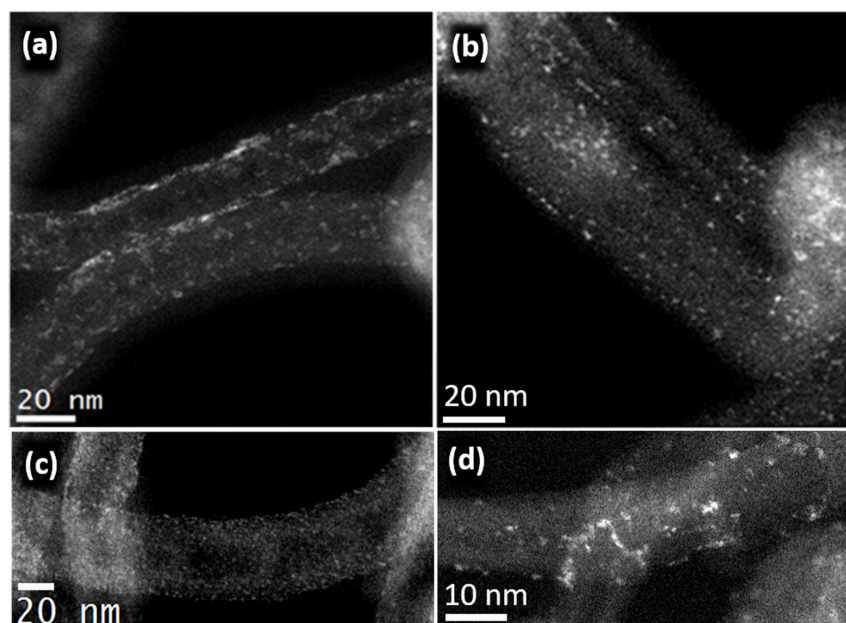


Figure 5. HAADF-STEM images of (a) 15 wt. % PW_4 /N-CNTs 1.8 at. % N, (b) 15 wt. % PW_4 /CNTs, (c) 8 wt. % PV_2W_{10} /N-CNTs (4.8 at. % N), and (d) 8 wt. % PV_2W_{10} /CNTs. Adapted with permission from ref. [100] Evtushok et al. Highly efficient catalysts based on divanadium-substituted polyoxometalate and N-doped carbon nanotubes for selective oxidation of alkylphenols *ACS Catalysis* **2018**, *8*, 1297–1307. Copyright 2018 American Chemical Society.

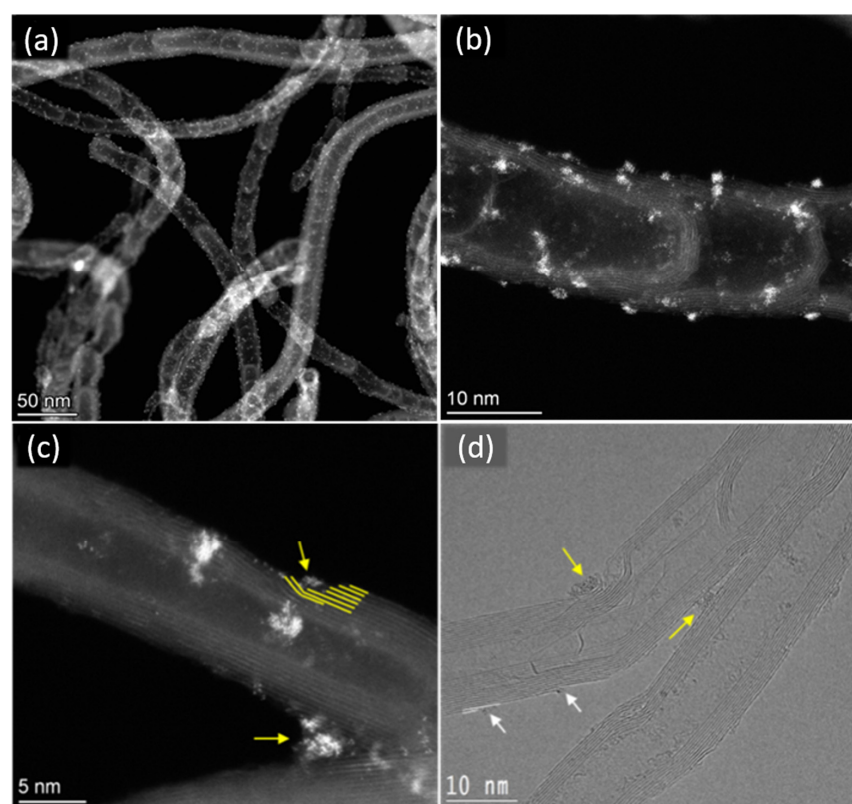


Figure 6. HAADF-STEM (a–c) and HRTEM (d) images of 8 wt. % NbW_5 /N-CNTs 4.8 at. % N (a,b) and 8 wt. % NbW_5 /CNTs (c,d). White arrows indicate a single POM species located near defects—cut-off edges of graphene layers exposed to the surface. Yellow arrows indicate POM agglomerates located on extended defects of CNTs surface and in the cavities between nanotubes. Reproduced from Ref. [103] with permission from the Royal Society of Chemistry.

Considering that defects are localized both in internal and external graphene layers [114], one can assume that the upper limit for POM adsorption is determined by the concentration of defects on the accessible (N)-CNTs surface.

Textural characteristics of POM/(N)-CNTs materials differ from the pristine (N)-CNTs by a slightly smaller surface area and pore volume [100–102]. Typical adsorption isotherms are shown in Figure 7.

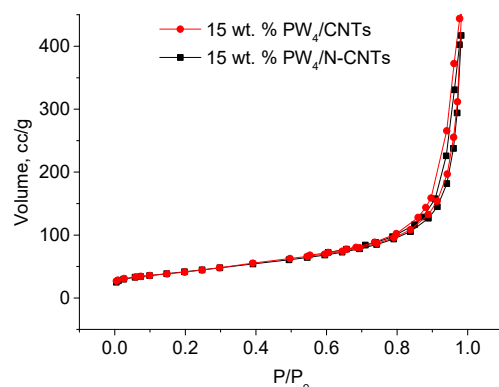


Figure 7. Nitrogen adsorption–desorption isotherms for 15 wt. % $PW_4/CNTs$.

IR spectroscopy is an important method for characterization of the POM state in POM/(N)-CNTs materials. However, obtaining the IR spectra of POM/(N)-CNTs is a rather difficult task since the nanotubes themselves strongly absorb in the entire IR range and the vibrations inherent in POMs stand out weakly against their background. In order to distinguish the vibrations of immobilized POM, it is necessary to consider the subtraction spectra. Although the resolution in the subtraction spectra is worse, it is possible to confirm reliably using IR spectroscopy that the structure of POM is retained after immobilization [100–103]. For PV_2W_{10} , some shift of the main absorption bands was observed, which can be associated with the electrostatic interaction of POM and (N)-CNTs. Interestingly, in the case of $NbW_5(L)$, the IR spectra look similar, regardless of which precursor was used to prepare the catalysts. The characteristic band of $Nb(O_2)$ at 600 cm^{-1} , as well as the splitting of the W-O-M bands, disappears after immobilization (Figure 8), indicating a reduction in the peroxy group. The key distinguishing feature of the dimeric $(NbW_5)_2O$, namely the Nb-O-Nb absorption band, also disappears upon immobilization (Figure 8). This allowed us to suggest that the stabilization of the monomeric form $[NbW_5(OH)O_{18}]^{2-}$ on the CNTs surface occurs, while the equilibrium is shifted towards the dimeric polyanion $[(NbW_5O_{18})_2O]^{4-}$ in the solution. The consequences of this monomer stabilization phenomenon for catalysis will be discussed in the next subsection.

2.2. Catalytic Activity of POM/(N)-CNTs in H_2O_2 -Based Oxidations

In mild conditions, N-free CNTs are not able to activate H_2O_2 and, as a result, show no activity in the oxidation of alkylphenols, alkenes, thioethers and most other organic substrates. This confirms the complete encapsulation of the residual metal catalyst employed during the CNTs synthesis within the carbon nanotubes and the absence of its effect on the catalytic properties. Nitrogen-doped carbon nanotubes, on the contrary, exhibit significant activity in the oxidation of organic compounds with H_2O_2 [100,101,103]. For example, Figure 9a shows how the conversion of cyclooctene increases with increasing N content in N-CNTs. However, the oxidation process is not selective as N-CNTs possess pronounced activity in the decomposition of hydrogen peroxide into water and molecular oxygen and the decomposition rate increases with the increase in the N content [100] (Figure 9b). So far, the mechanism of H_2O_2 activation on N-CNTs remains unstudied. We cannot exclude the role of surface defects (see above) in this process. Therefore, it makes sense to use either N-CNTs with a relatively small amount of nitrogen or undoped CNTs as supports

for H_2O_2 -based oxidation catalysis. Below, we will try to demonstrate how the choice of support can tune the catalytic performance of POM/(N)-CNTs.

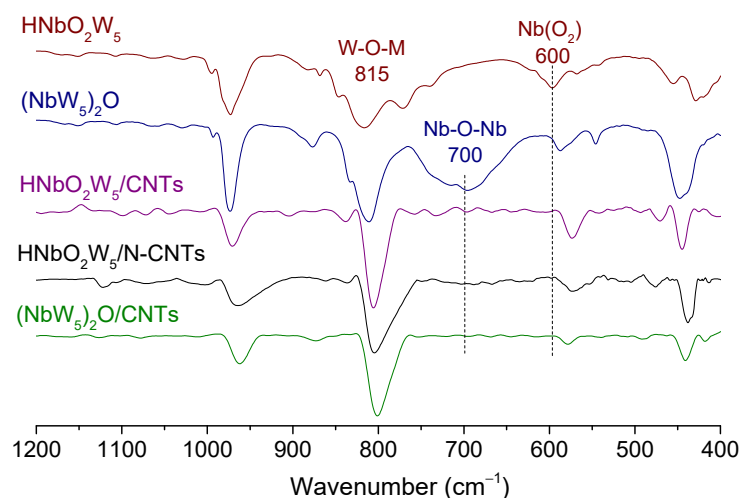


Figure 8. FTIR spectra of $\text{TBA}_2[\text{HNbW}_5(\text{O}_2)\text{O}_{18}]$, $\text{TBA}_4[(\text{NbW}_5\text{O}_{18})_2\text{O}]$, 15 wt. % $[\text{HNbW}_5(\text{O}_2)\text{O}_{18}]/\text{CNTs}$, 15 wt. % $[\text{HNbW}_5(\text{O}_2)\text{O}_{18}]/\text{N-CNTs}$ (0.9 at. % N), and 15 wt. % $[(\text{NbW}_5\text{O}_{18})_2\text{O}]/\text{CNTs}$ (spectrum of (N)-CNTs was subtracted). Reproduced from Ref. [103] with permission from the Royal Society of Chemistry.

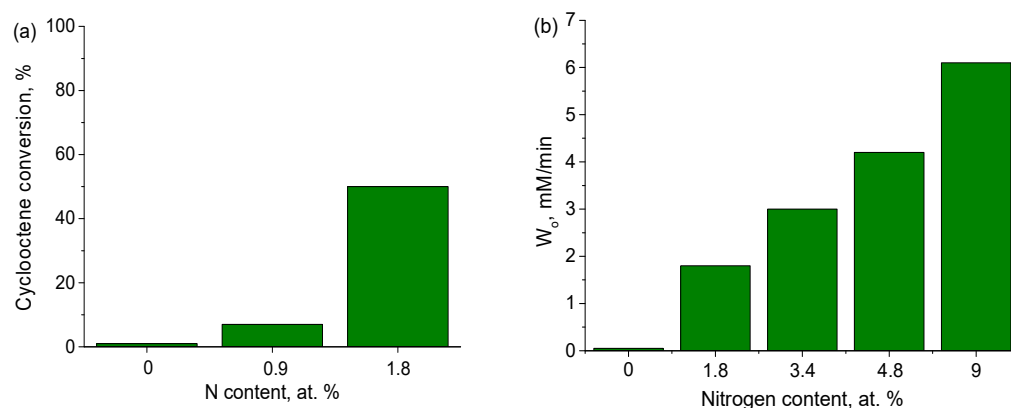


Figure 9. Effect of N content in N-CNTs on (a) cyclooctene conversion in the oxidation with H_2O_2 over N-CNTs ($[\text{CyO}] = 0.1 \text{ M}$, $[\text{H}_2\text{O}_2] = 0.1 \text{ M}$, 10 mg of N-CNTs, 5 mL CH_3CN , 4 h, 50°C) and (b) initial rate (W_0) of H_2O_2 decomposition in the absence of organic substrate ($[\text{H}_2\text{O}_2] = 0.11 \text{ M}$, 10 mg N-CNTs, 5 mL CH_3CN , 50°C).

2.2.1. Alkene Oxidation

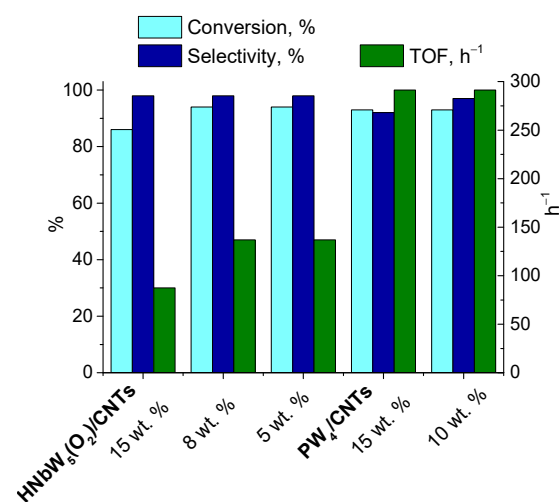
High activity of POM/(N)-CNTs catalysts in the selective oxidation of alkenes with 30% aqueous H_2O_2 has been demonstrated for a range of POMs [101–103]. Table 3 summarizes data on the oxidation of cyclooctene (CyO) and cyclohexene (CyH) over (N)-CNTs-immobilized PV_2W_{10} , NbW_5 , and PW_4 . This pair of olefin substrates was chosen as CyO epoxide is very stable against acid-catalyzed epoxide ring-opening, while cyclohexene epoxide is oppositely sensitive. In addition, CyH is susceptible to one-electron allylic oxidation as it possesses highly reactive H atoms in the allylic position. This feature of CyH allows one to employ it as a model substrate for evaluation of the contribution of homolytic and heterolytic pathways to the activation of H_2O_2 [115]. Thus, the oxidation of CyO facilitates the identification of factors affecting the activity of catalysts, whereas the oxidation of CyH reveals factors affecting selectivity.

Table 3. Catalytic performance of POM/(N)-CNTs in H₂O₂-based oxidation of CyO and CyH in comparison with homogeneous POM (the data taken from refs. [101–103]).

Catalyst	POM wt. %/H ⁺ Added equiv. ^a	Conversion CyO/CyH, %	Epoxide Selectivity CyO/CyH, %	<i>trans</i> -Cyclohexane Diol Selectivity, %	TOF CyO/CyH, h ⁻¹	Catalyst Recycling
TBA _{3.5} [H _{1.5} PV ₂ W ₁₀ O ₄₀]	-	-/93	-/94	5	-/341	+
PV ₂ W ₁₀ /N-CNTs ^b	15/1	-/39	-/51	33	-/147	n.d. ^c
PV ₂ W ₁₀ /CNTs	15/1	-/82	-/79	19	-/310	-
TBA ₂ [HNbW ₅ (O ₂)O ₁₇]	-	20/30	80/5	53	12/-	+
NbW ₅ /N-CNTs ^d	15/2	70/30	97/23	38	59/72	+
NbW ₅ /CNTs	15/2	86/59	98/15	55	96/58	+
NbW ₅ /CNTs	8/2	94/-	98/-	-	139/-	+
NbW ₅ /CNTs	10/0	63/32	99/39	43	42/-	+
THA ₃ [PW ₄ O ₂₄]	-	80/90	100/77	16	44/-	+
PW ₄ /N-CNTs ^b	15/1	37/-	89/-	-	136/-	+
PW ₄ /CNTs	15/2	93/82	97/2	90	290/410	+/- ^e
PW ₄ /CNTs	5/0	82/46	98/82	15	41/40	+

^a HClO₄ added during catalyst preparation. ^b 1.8 at. % N; ^c Not determined; ^d 0.9 at. % N; ^e Activity gradually decreased; Reaction conditions: [Substrate] = 0.1 M, [H₂O₂] = 0.1 M for CyH or 0.2 M for CyO. PV₂W₁₀ 1.3 μmol, CH₃CN 1 mL, 30 °C. NbW₅ 0.8 μmol, solvent 1 mL (DMC for NbW₅/(N)-CNTs, CH₃CN for TBA₂[HNbW₅(O₂)O₁₇]), 50 °C. PW₄ 0.7 μmol, solvent 1 mL (DMC for PW₄/(N)-CNTs, CH₃CN for THA₃[PW₄O₂₄]), 50 °C.

If we consider the data on the dependence of the catalytic activity of POM/(N)-CNTs on the POM content, we can see that no change in the specific activity (turnover frequency determined from the initial rates, TOF) is observed for the PW₄/CNTs catalysts, while the activity of NbW₅/CNTs decreases with an increase in the POM content above 8 wt. % (Figure 10). Such a drop in the activity of the NbW₅/CNTs catalysts can be interpreted by the aggregation of this POM on the surface, which was also confirmed by the HAADF-STEM method [103]. On the other hand, the catalytic data corroborate that PW₄ is well dispersed on the surface of CNTs up to, at least, 15 wt. % of POM.

**Figure 10.** CyO epoxidation over PW₄/CNTs and NbW₅/CNTs with various POM content. Reaction conditions: [CyO] = 0.1 M, [H₂O₂] = 0.2 M, catalyst 10–30 mg (0.7 μmol PW₄ or 0.8 μmol NbW₅), DMC 1 mL, 50 °C.

Activity of POM/(N)-CNTs catalysts expressed in TOF values follows the same order as activity of the corresponding homogeneous POMs and decreases in the series PV₂W₁₀ > PW₄ > NbW₅ (Table 3). More importantly, activity of (N)-CNTs-immobilized POM in the oxidation of alkenes is generally superior or, at least, similar to activity of their soluble salts.

This is a quite unusual phenomenon as activity of most supported POM-based catalysts is either similar or lower than that of soluble POM salts [37,44,52,54]. Several reasons that may account for this phenomenon will be discussed below.

One of possible reasons for the enhanced activity of the POM/CNTs catalysts can be related to their acidity. With an increase in the amount of HClO₄ added during the catalyst preparation, activity of POM/CNTs in the alkene oxidation increases markedly (see Table 3). The same tendency was observed for homogeneous POM. As a working hypothesis, it can be tentatively explained by a higher electrophilicity of protonated POM peroxo complexes [116,117]. Indeed, activity of PW₄/CNTs prepared without acid is close to that of homogeneous PW₄. The degree of POM protonation may not be the only explanation for the increased activity of the catalysts. In particular, deprotonation of POM and redistribution of protons is likely to occur in the presence of aqueous H₂O₂ as water is a weak base and can compete with POM for protons. On the other hand, protonation of the surface of nanotubes withdraws the electron density from defects [106] and can indirectly reduce the electron density on POMs, which might give an effect similar to direct POM protonation. Another possible activity-enhancing factor is the preferential adsorption of substrate and oxidant on the support, leading to an increase in the local concentration of the reagents and thereby increasing the reaction rate. In the case of the NbW₅/CNTs catalysts, an additional factor that may strongly improve catalytic activity is the stabilization of the monomeric form of this POM on the surface of CNTs [103], that was discussed in Section 2.1.

Interestingly, POM/N-CNTs, in general, demonstrate intermediate activity between the POM/CNTs catalysts prepared with and without acid. For example, in the epoxidation of cyclooctene, 15 wt. % PW₄/N-CNTs shows the value of TOF 136 h⁻¹, which lays between TOF 290 and 41 h⁻¹ for 15 wt. % PW₄/CNTs (2 equiv. H⁺) and 5 wt. % PW₄/CNTs (0 equiv. H⁺), respectively (Table 3). This might be explained by the fact that protonation of N-CNTs would give weaker conjugate acids due to the presence of basic N-groups than protonation of CNTs, which contain only weakly basic O-groups.

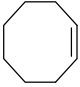
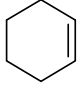
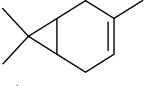

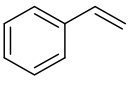
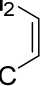
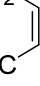
It is worth noting an important point in the oxidation of cyclohexene over POM/(N)-CNTs, namely, the incomplete conversion of the substrate in the presence of the stoichiometric amount of H₂O₂. The unproductive decomposition of H₂O₂ is partially responsible for that, especially, in the case of N-CNTs. Indeed, our studies showed that an increase in the N content in N-CNTs leads to a sharp decline in the catalyst efficiency as a result of the enhancement of the unproductive decomposition of H₂O₂ [100,103]. Meanwhile, the oxidant utilization efficiency of POM/CNTs catalysts in the oxidation of alkenes is, in general, high (e.g., >90% for PW₄/CNTs). Presumably, POM binding with cyclohexene oxide and/or *trans*-cyclohexane-1,2-diol [118] and preferential adsorption of the oxidation products on the surface is responsible for the catalyst deactivation during the reaction.

Clearly, an increase in the amount of acid in the POM/CNTs catalysts produces a negative effect on selectivity to CyH epoxide (selectivity to acid-insensitive CyO epoxide remains high) which transforms to *trans*-cyclohexane-1,2-diol, a product of acid-catalyzed epoxide ring-opening. This transformation can be counterbalanced by either increasing concentration of the H₂O₂ reactant (e.g., by taking 50 or 70% H₂O₂ instead of the 30% one), or enhancing catalyst hydrophobicity [119,120], or adding Lewis bases [76,121]. More significantly, the total selectivity toward heterolytic oxidation products, epoxide and diol, is high and can reach 98% (Table 3).

The POM/(N)-CNTs catalysts can be used for selective epoxidation of a broad spectrum of alkenes with H₂O₂, provided an optimal support/catalyst preparation method is employed. The effect of N-doping on the epoxide selectivity/yield strongly depends on the specific alkene substrate. While, for CyO, high epoxide selectivity can be reached over both POM/N-CNTs and POM/CNTs, N-free CNTs are preferable as supports in case of CyH (see Table 3). In general, higher yields of epoxides can be attained with POM/CNTs than with POM/N-CNTs.

Table 4 presents catalytic oxidation of various alkenes over $PW_4/CNTs$ in dimethyl carbonate (DMC). Along with CH_3CN , this solvent allows the production of epoxides with high yields, whereas the use of polar protic solvents, e.g., CH_3OH , drastically decreases the catalyst activity and attainable substrate conversion, probably, due to competition with H_2O_2 for the active sites [101]. On the other hand, DMC showed advantages over CH_3CN in terms of the catalyst stability toward POM leaching (this matter will be discussed in Section 2.3).

Table 4. Catalytic oxidation of various alkenes with H_2O_2 over $PW_4/CNTs$ catalysts.

Substrate	Catalyst	$HClO_4$ Added, equiv. ^a	Time, h	Conversion, %	Selectivity, %
	15 wt. % $PW_4/CNTs$	2	2	93	97
	5 wt. % $PW_4/CNTs$	0.2	4	66	79
	5 wt. % $PW_4/CNTs$	0	5	50	80
	15 wt. % $PW_4/CNTs$	2	1	100	65
	5 wt. % $PW_4/CNTs$	0	7	14	95
$CH_3(CH_2)_6CH_2$ 	5 wt. % $PW_4/CNTs$	0	4	85	85
$MeO_2C(H_2C)_6H_2C$ 	5 wt. % $PW_4/CNTs$	0	4	85	85

^a $HClO_4$ added during catalyst preparation. Reaction conditions: [Substrate] = 0.1 M, $[H_2O_2]$ = 0.1 M, catalyst 10–30 mg (0.7 μ mol PW_4), DMC 1 mL, 50 °C.

While high yields of epoxides can be reached with the acid-prepared $PW_4/CNTs$ catalysts for such substrates as CyO or the bulky terpene, caryophyllene, acid-free catalysts show superior results, in terms of selectivity, for alkenes with epoxides prone to ring-opening (Table 4). Given that protons promote the catalyst activity, a careful balance between activity and selectivity should be struck. Tuning the amount of acid in the catalyst synthesis can be a useful tool in reaching such balance.

A comparison of the catalytic performance of the acid-free 5 wt. % PW_4/CNT catalyst with the results reported in the literature for other heterogeneous phosphotungstate-based catalysts in the epoxidation of the challenging substrate CyH with 30% H_2O_2 is given in Table 5.

Among the reported catalysts, 5 wt. % PW_4/CNT demonstrates a rather high activity per W (6 h^{-1}), especially considering that its activity was measured at 50 °C. Epoxide selectivity (79%) and alkene conversion (66%) are comparable to homogeneous PW_4 in similar conditions [61]. It is most likely that these characteristics can be improved by optimizing the reaction conditions, for example by using more concentrated H_2O_2 . It has also been shown that 5 wt. % PW_4/CNT can be reused for at least four cycles without decline in activity, selectivity and conversion. The absence of leaching and heterogeneous nature of the catalysis over 5 wt. % PW_4/CNT was confirmed by a hot filtration test and ICP-OES analysis of the filtrate (a detailed discussion on the catalyst stability and reusability will be given in Section 2.3).

Table 5. Comparison of the catalytic performance of 5 wt. % PW_4/CNT with other reported heterogeneous catalysts based on phosphotungstates in CyH epoxidation.

Catalyst	CyH:H ₂ O ₂ :W mol:mol:mol	Solvent	T °C	t h	Conv. %	Epoxy. Select. %	TON ^a	TOF ^b h ⁻¹
5% $PW_4/CNTs$ [101]	36:36:1	DMC	50	4	66	79	24	6
$PW_{12}/MIL-101$ [61]	17:34:1	CH ₃ CN	50	3	72	76	12	4
$PW_x/phosp-MCM-41$ [76]	80:120:1	CH ₃ CN	50	20	30	60	24	1.2
$PW_x/D201$ resin [55]	22:26.5:1	CH ₃ CN	50	6	92	98	22	3.7
PW_4/NH_2-AC [58]	200:300:1	CH ₃ CN	80	24	63	99	126	5
PW_{12}/SPC [51]	50:120:1	CH ₃ CN	80	4	99	75	49	12

^a TON = (mol of epoxide produced)/mol of W atoms. ^b Since data on initial rates are not available in the literature, here we use for comparison the values of $TOF_{average} = TON / \text{reaction time}$.

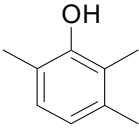
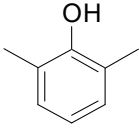
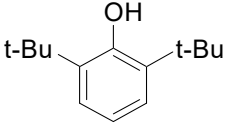
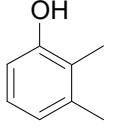
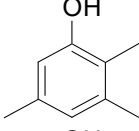
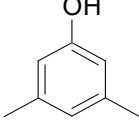
As one can judge from the data provided in Table 5, the highest epoxide selectivity of 98% at 92% CyH conversion was reported for CyH epoxidation over $PW_x/D201$ resin [55]. The reusability of catalysts $PW_x/D201$ resin [55], PW_4/NH_2 -groups modified activated carbon (PW_4/NH_2-AC) [58] and $PW_{12}/silica$ -pillared clay (PW_{12}/SPC) [51] was shown to be successful. However, important data on the retention of activity [122] between operation cycles were not provided. Moreover, leaching was found for PW_4/NH_2-AC (<5% after four cycles) and a hot filtration test was not conducted to verify the nature of the observed catalysis. In turn, leaching was declared to be minimal for PW_{12}/SPC , but without providing experimental evidence [51]. Tungsten peroxy species immobilized on a mesostructured silicate MCM-41 through a covalently linked phosphoramidate group revealed the truly heterogeneous nature of the catalysis and minor tungsten leaching (<2%); however, experiments on the reuse of $PW_x/phosp-MCM-41$ were not reported [76]. Therefore, we may conclude that, based on the combination of all characteristics, including activity, selectivity, productivity, resistance to leaching, and good recyclability (the latter will be discussed in more detail in Section 2.3), the catalyst 5% $PW_4/CNTs$ can be considered quite promising for epoxidation reactions.

2.2.2. Alkylphenol Oxidation

As in the case of alkenes, POM-free N-CNTs are able to catalyze the oxidation of phenols, in particular, 2,3,6-trimethylphenol (TMP). However, the target oxidation product trimethyl-*p*-benzoquinone (TMBQ, Vitamin E precursor) cannot be produced. Instead, the main oxidation product formed over N-CNTs is the corresponding bisphenol [100]. Use of $PV_2W_{10}/(N)$ -CNTs catalysts change the reaction selectivity drastically [100,102]. The catalyst $PV_2W_{10}/CNTs$ turned out to be as selective as homogeneous PV_2W_{10} [100], but it was prone to POM leaching already in mild reaction conditions [102]. In contrast, the PV_2W_{10}/N -CNTs materials proved to be highly efficient catalysts for the oxidative conversion of alkylphenols to the corresponding *p*-benzoquinones, using 30% aqueous H₂O₂ (Table 6). The exception was *m*-substituted alkylphenols, for which low conversions were found, most likely, due to the high steric hindrance of the active vanadium peroxy complex [123,124].

Like in the oxidation of alkenes, an increase in the amount of N in N-CNTs strongly deteriorated the oxidant utilization efficiency [100]. With the optimal catalyst 15 wt. % PV_2W_{10}/N -CNTs (1.8 at. % N), TMBQ could be produced in the yield as high as 99%, with 80% oxidant efficiency. In addition, the catalyst revealed unprecedentedly high activity ($TOF = 500 \text{ h}^{-1}$) and productivity ($STY = 450 \text{ g L}^{-1} \text{ h}^{-1}$) (Figure 11).

Table 6. Oxidation of various alkylphenols with H₂O₂ catalyzed by 15 wt. % PV₂W₁₀/N-CNTs (1.8 at. % N). Adapted with permission from ref. [100] Evtushok et al. Highly efficient catalysts based on divanadium-substituted polyoxometalate and N-doped carbon nanotubes for selective oxidation of alkylphenols *ACS Catalysis* 2018, 8, 1297–1307. Copyright 2018 American Chemical Society.

Substrate	Conversion, %	Selectivity, %	Quinone Yield, %
	100	99	99
	90	90	81
	94	90	85
	30	88	26
	15	10	2
	10	0	0

Reaction conditions: [Substrate] = 0.1 M, [H₂O₂] = 0.45 M, 15 wt. % PV₂W₁₀/N-CNTs 1.8 at. % N catalyst 40 mg (1.6 μmol PV₂W₁₀), CH₃CN 1 mL, 15 min, 60 °C.

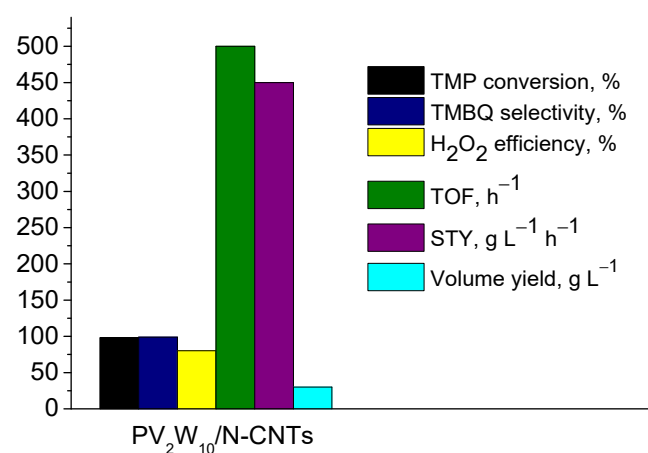


Figure 11. Catalytic characteristics of PV₂W₁₀/N-CNTs in TMP oxidation to TMBQ with H₂O₂. (STY: space-time yield). Adapted with permission from ref. [100] Evtushok et al. Highly efficient catalysts based on divanadium-substituted polyoxometalate and N-doped carbon nanotubes for selective oxidation of alkylphenols *ACS Catalysis* 2018, 8, 1297–1307. Copyright 2018 American Chemical Society.

In Table 7, we give a comparison of the catalytic performance of PV₂W₁₀/N-CNTs with the homogeneous catalyst, TBA-salt of PV₂W₁₀, and various solid PV₂W₁₀ catalysts prepared by other methodologies. Supports that provide electrostatic binding of POM,

such as MIL-101 and NH₂-SiO₂, do not allow high conversions and selectivity characteristics of homogeneous PV₂W₁₀ to be achieved. An explanation for this fact can be found in the strong effect of the PV₂W₁₀ protonation state on its catalytic properties in H₂O₂-based oxidations. Thus, for effective oxidation of TMP, it must be, at least, in the monoprotonated state [γ-PW₁₀O₃₈V₂(μ-O)(μ-OH)]⁴⁻ [125], while the diprotonated form [γ-PW₁₀O₃₈V₂(μ-OH)(μ-OH)]³⁻ has even higher activity [123,124,126]. Strong electrostatic binding of PV₂W₁₀ with NH₂-SiO₂ or MIL-101 may lead to deprotonation of the polyanion, resulting in the catalytically inactive form [γ-PW₁₀O₃₈V₂(μ-O)₂]⁵⁻. Other factors, first of all, those related to adsorption of reagents and/or products may also affect the activity of supported PV₂W₁₀. Catalysts prepared by PV₂W₁₀ encapsulation within SiO₂ pores by the sol-gel methodology or adsorption on the carbon support Sibunit are able to carry out TMP oxidation more efficiently in terms of attainable TMP conversion and TMBQ selectivity. However, PV₂W₁₀@SiO₂ acts as a homogeneous rather than a heterogeneous catalyst due to the leaching of a large amount of PV₂W₁₀ during the oxidation process. The Sibunit-supported PV₂W₁₀ was stable to POM leaching, but it demonstrated a rapid loss of catalytic characteristics as a result of strong adsorption of the oxidation products on the carbon surface. Already in the second run, TMBQ selectivity and TMP conversion were only 23% and 50%, respectively. Treatments with boiling solvents, CH₃CN and CH₃OH, did not help in restoring the initial catalytic performance. Therefore, we can conclude that N-CNTs are unique supports for the immobilization of PV₂W₁₀ in relation to the production of alkyl-*p*-benzoquinones and other oxidation reactions, where the retention of the POM protonation state is crucial.

Table 7. TMP oxidation with H₂O₂ over various PV₂W₁₀-based catalysts.

Catalyst	TMP Conversion, %	TMBQ Selectivity, %	TMBQ Yield, %
TBA ₄ [HPV ₂ W ₁₀ O ₄₀]	100	99	99
PV ₂ W ₁₀ /N-CNTs	100	99	99
PV ₂ W ₁₀ /MIL-101	22	68	15
PV ₂ W ₁₀ /NH ₂ -SiO ₂	68	68	46
PV ₂ W ₁₀ /Sibunit	86 (50) ^a	90 (23) ^a	77 (11)
PV ₂ W ₁₀ @SiO ₂	98 ^b	98	96

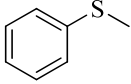
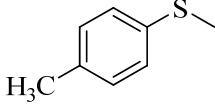
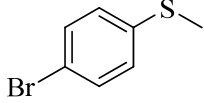
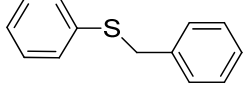
Reaction conditions: 0.1 M TMP, 0.35 M H₂O₂, catalyst 40–60 mg (1.5 mM PV₂W₁₀), 1 mL CH₃CN, 15 min, 60 °C.

^a After first cycle; ^b PV₂W₁₀ leaching (ca. 15%).

2.2.3. Thioethers Oxidation

Successful oxidation of a range of thioethers with H₂O₂ could be accomplished using PW₄/CNTs catalysts (Table 8). Acetonitrile was found to be the solvent of choice for this reaction [101]. In the oxidation of methyl phenyl sulfide (MPS) over PW₄/CNTs, selectivity to methyl phenyl sulfoxide (MPSO) was similar to that of homogeneous PW₄, but catalyst activity was lower. In contrast to the epoxidation reactions, catalytic activity decreased with an increase in the amount of acid in the catalysts. A decrease in activity with the addition of acid was also observed for the homogeneous catalyst THA-PW₄. This might be caused by protonation of the thioether and, thereby, decreasing its nucleophilicity and, in turn, reactivity towards electrophilic oxidizing species. On the other hand, catalyst acidity favors the formation of sulfoxide over sulfone, most likely, due to the increasing electrophilicity of active peroxo species upon protonation [116]. Therefore, it can be seen again that a balance between the catalyst activity and selectivity is required.

Table 8. Catalytic oxidation of various thioethers with H₂O₂ over PW₄/CNTs catalysts.

Substrate	Catalyst/ $\mu\text{mol PW}_4$	HClO ₄ Added ^a , equiv.	Time, h	Thioether conv., %	Sulfoxide Selectivity, %
	THA ₃ [PW ₄ O ₂₄]/1	0	0.25	93	83
	THA ₃ [PW ₄ O ₂₄]/1	1	0.5	92	86
	15 wt. % PW ₄ /CNTs/1	2	2.5	93	90
	15 wt. % PW ₄ /CNTs/0.3	2	6	93	92
	5 wt. % PW ₄ /CNTs/0.3	0	3	88	84
	15 wt. % PW ₄ /CNTs/1	2	2	90	88
	15 wt. % PW ₄ /CNTs/1	2	2	94	89
	15 wt. % PW ₄ /CNTs/1	2	2	86	81

^a HClO₄ added during catalyst preparation or added in reaction mixture in case of homogeneous PW₄. Reaction conditions: [Substrate] = 0.1 M, [H₂O₂] = 0.1 M, catalyst 15 mg (0.3–1 $\mu\text{mol PW}_4$), CH₃CN 1 mL, 27 °C.

2.3. Catalyst Stability and Reusability

The choice of an optimum catalyst for the particular selective oxidation processes should be conducted taking into account its stability and reusability under the reaction conditions. The important aspect of catalyst stability is the preservation of the POM structure under turnover conditions. It was shown by IR spectroscopy that the key absorption bands of POM remain intact in the spectra of (N)-CNTs-supported POM after catalysis (Figure 12). In addition, both IR and XPS spectra confirmed that (N)-CNTs themselves are not oxidized under the employed conditions of liquid-phase oxidation [100].

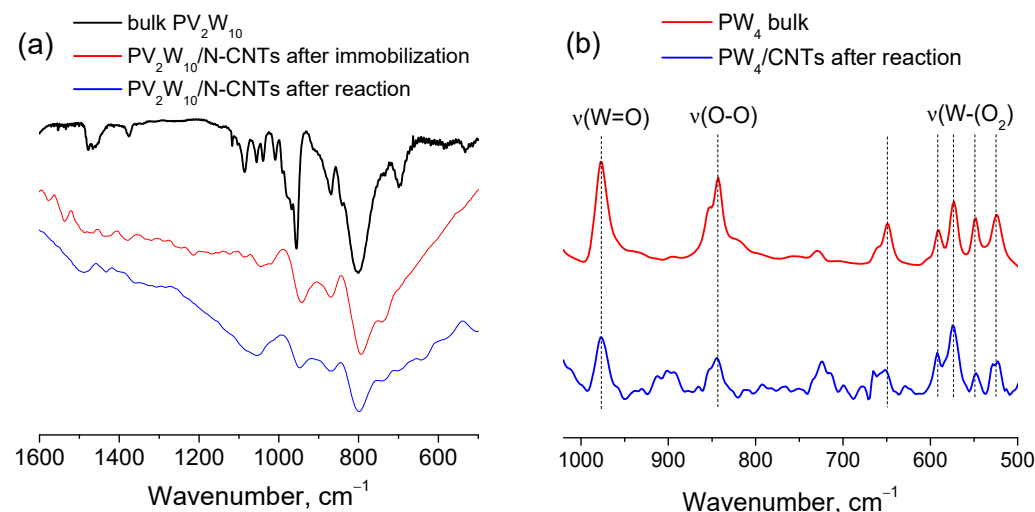


Figure 12. FT-IR spectra of (a) bulk PV₂W₁₀, 8 wt. % PV₂W₁₀/N-CNTs, and 8 wt. % PV₂W₁₀/N-CNTs after 2,3,6-trimethylphenol oxidation and (b) bulk PW₄ and 15 wt. % PW₄/CNTs catalyst after cyclooctene oxidation (the spectra of (N)-CNTs were subtracted).

Studies on POM/(N)-CNTs stability demonstrated that POM leaching into solution strongly depends on the specific oxidation reaction and its conditions, in particular, the choice of solvent [100–103]. If CH₃CN is used as the reaction medium for alkene epoxidation, the POM/CNTs catalysts prepared without acid undergo complete leaching of POM,

while $PW_4/CNTs$ and $PV_2W_{10}/CNTs$ prepared with acid are subject to slight leaching (25–35 ppm of W) [101,102].

Hot filtration tests demonstrated the truly heterogeneous nature of the observed catalysis and, coupled with elemental analysis of the filtrates, proved that $PW_4/CNTs$ and $NbW_5/CNTs$ are not susceptible to POM leaching during epoxidation if DMC is employed as the solvent (Figure 13).

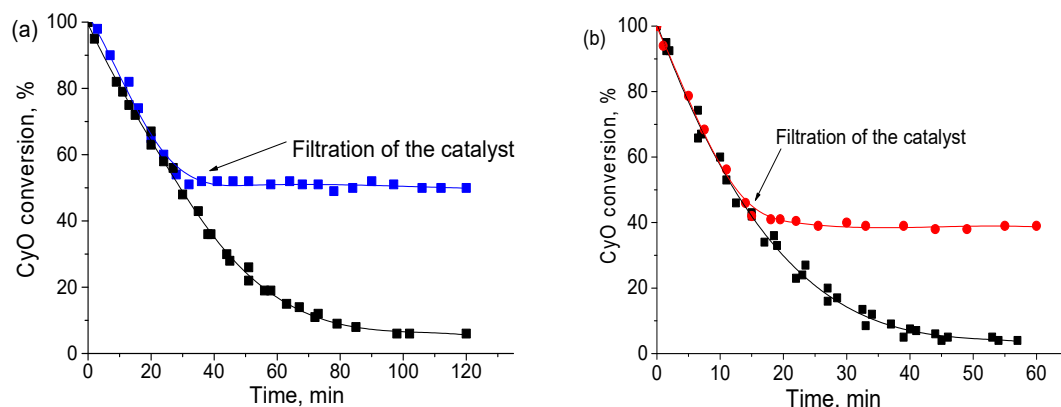


Figure 13. Hot catalyst filtration test for CyO oxidation with H_2O_2 over (a) 15 wt. % $NbW_5/CNTs$ and (b) 15 wt. % $PW_4/CNTs$. Reaction conditions: $[CyO] = 0.1$ M, $[H_2O_2] = 0.2$ M, 15 wt. % POM/CNTs 10 mg (0.7 μ mol PW_4 , 0.8 μ mol NbW_5), DMC 1 mL, 50 °C.

Evaluation of the 15 wt. % $PW_4/CNTs$ and 15 wt. % $NbW_5/CNTs$ catalysts prepared with acid under more severe conditions (0.8 M H_2O_2 , CH_3CN , 80 °C) showed that the filtrate remaining after the separation of $PW_4/CNTs$ and $NbW_5/CNTs$ contained ca. 50% of the initial amount of POM. On the other hand, the catalysts 15 wt. % $PW_4/N-CNTs$ and 15 wt. % $NbW_5/N-CNTs$ demonstrated fairly good stability under a similar treatment: only 0.04% and 2% of POM, respectively, were found in the filtrate. Therefore, we may conclude that POMs are more strongly bound to N-CNTs than to CNTs, and the corresponding POM/N-CNTs catalysts are less prone to leaching and are able to withstand more severe reaction conditions. Indeed, under the conditions employed for the alkylphenol oxidation (0.35 M H_2O_2 , CH_3CN , 60 °C), the $PV_2W_{10}/N-CNTs$ catalysts, in contrast to $PV_2W_{10}/CNTs$, revealed the truly heterogeneous nature of the catalysis and suffered no leaching [100]. Therefore, the presence of N in CNTs is certainly crucial for the stability of the supported POM catalysts.

The possibility of recycling the POM/(N)-CNT catalysts in the selective oxidation of alkenes, thioethers, and alkylphenols has been demonstrated [100–103]. In almost all cases, the preservation of catalytic characteristics in several consecutive operation cycles was observed, provided the catalysts were optimally regenerated. Thus, during the recycling of the 15 wt. % $PW_4/CNTs$ catalyst in CyO epoxidation in DMC, a progressive decline in activity was observed that was related to the loss of the catalyst acidity during the catalysis. However, the catalyst could be cured by an acid treatment. Indeed, Figure 14a demonstrates that successful regeneration of 8 wt. % $NbW_5/CNTs$ after the catalytic reaction in DMC was fulfilled by treatment with an $HClO_4$ solution. At the same time, the acid-free catalyst 5 wt. % $PW_4/CNTs$ could be regenerated by simple filtration and washing with DMC (Figure 14b).

Under the conditions of alkylphenol oxidation, the catalyst 15 wt. % $PV_2W_{10}/N-CNTs$ (1.8 at. % N) demonstrated excellent stability [100]. The catalyst could be reused, at least six times, without appreciable losses of activity and selectivity (Figure 15a).

Recycling experiments with 15 wt. % $PW_4/CNTs$ in the MPS oxidation also showed the retention of catalytic characteristics after, at least, three reuses [101] (Figure 15b). However, it was necessary to wash the catalyst with DMC after separation from the reaction mixture

to preserve its catalytic characteristics. Washing the catalyst with CH_3CN did not fully restore the activity [101].

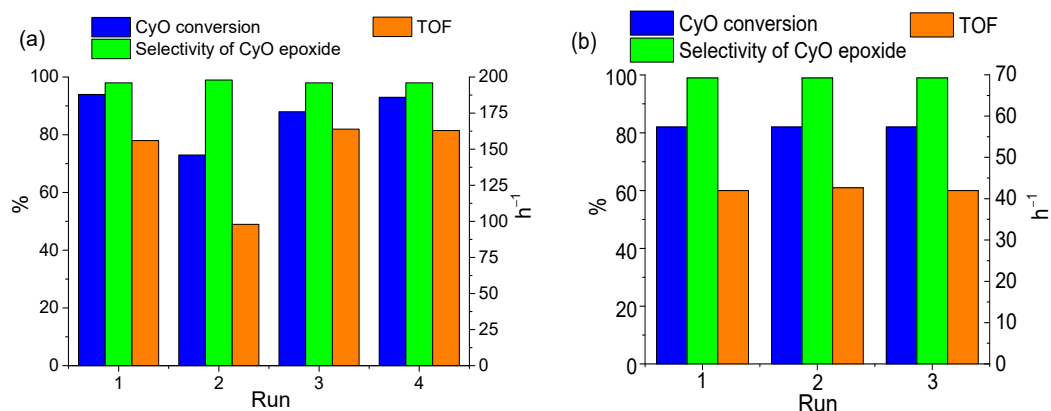


Figure 14. Reusability of the catalysts (a) 8 wt. % NbW_5/CNTs and (b) 5 wt. % PW_4/CNTs in CyO epoxidation. Reaction conditions: $[\text{CyO}] = 0.1 \text{ M}$, $[\text{H}_2\text{O}_2] = 0.2 \text{ M}$, 20–30 mg catalyst (0.7 μmol PW_4 , 0.8 μmol NbW_5), DMC 1 mL, 50 °C. The catalyst 8 wt. % NbW_5/CNTs was treated with HClO_4 in CH_3CN (2 equiv. to POM) after the second and subsequent runs. a) Adapted from ref. [103] with permission from the Royal Society of Chemistry.

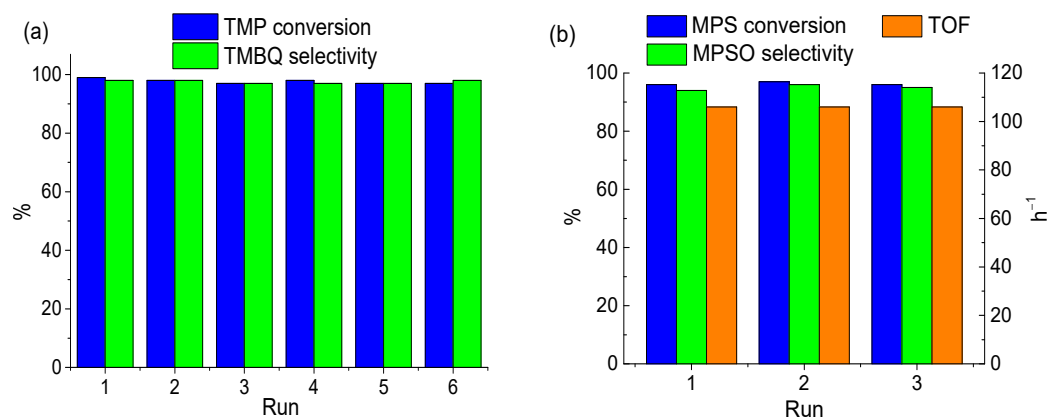


Figure 15. Recycling of (a) 15 wt. % $\text{PV}_2\text{W}_{10}/\text{N-CNTs}$ (1.8 at. % N) in TMP oxidation ($[\text{TMP}] = 0.1 \text{ M}$, $[\text{H}_2\text{O}_2] = 0.45 \text{ M}$, catalyst 40 mg (1.6 μmol PV_2W_{10}), CH_3CN 1 mL, 15 min, 60 °C) and (b) 15 wt. % PW_4/CNTs in MPS oxidation ($[\text{MPS}] = 0.1 \text{ M}$, $[\text{H}_2\text{O}_2] = 0.1 \text{ M}$, catalyst 15 mg (1 μmol PW_4), CH_3CN 1 mL, 27 °C).

3. Conclusions and Outlook

In this short perspective paper, we tried to demonstrate that both N-doped and undoped CNTs are prospective supports for the immobilization of POMs, having high catalytic activity in selective oxidations with aqueous hydrogen peroxide. The main factors that ensure irreversible adsorption of POMs on N-CNTs and CNTs are the preliminary drying of the supports and additives of mineral acid (HClO_4). The elaborated approach to POM immobilization compares favorably with simple impregnation by the high stability of the materials obtained. On the other hand, it is much less laborious than the covalent bonding of POM to CNTs or the preliminary modification of CNTs with ion-exchange groups.

A simplified representation of the effects of protons and N-doping on POM adsorption on CNTs and catalytic properties of the immobilized POM is given in Figure 16. However, the effect of N-doping on the dispersion of POMs on the surface of nanotubes strongly depends on the POM nature. While the presence of N certainly favors the quasi molecular dispersion of classic POMs of the Keggin and Lindqvist structures, it may produce the opposite result in the case of the immobilization of low nuclearity species, such as the

Venturello complex. A different type of binding between the POM and N species might be responsible for that.

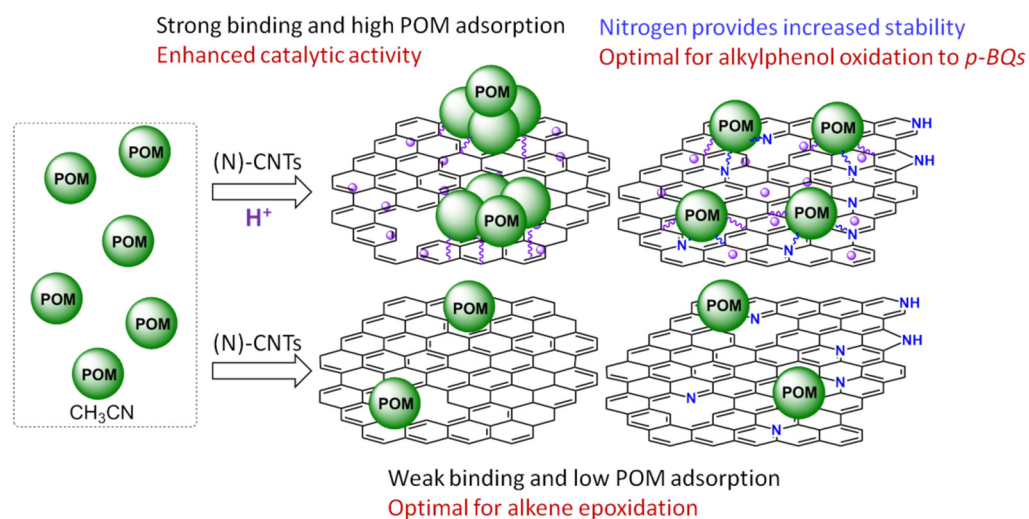


Figure 16. A simplified representation of the effects of protons and N-doping on POM adsorption on CNTs and catalytic properties of immobilized POM.

Catalytic studies have shown that (N)-CNTs-supported POMs have high activity, selectivity and stability in various selective oxidations with 30% aqueous H_2O_2 . In general, their catalytic activity is superior or, at least, similar to that of the corresponding homogeneous POMs. (N)-CNTs enable the stabilization of most active monomeric forms of POM and may allow the protonation state of POM upon immobilization to be kept. The proper choice of POM, support (N-free or N-doped) and immobilization technique (with or without the addition of acid) depends on the oxidation reaction and, moreover, may depend on the specific organic substrate. While N-doping and the use of acid during the catalyst preparation certainly play a positive role in the oxidation of alkylphenols to the corresponding *p*-benzoquinones, N-free and acid-less supports often show advantages if we deal with the epoxidation of alkenes. From the viewpoint of catalyst stability, the presence of N in the support undoubtedly endows the strong binding of POM and prevents its leaching. However, if N-free supports are preferable to ensure oxidation selectivity (e.g., in alkene epoxidation), a proper choice of solvent (e.g., the use of DMC) may help in solving the problem of POM leaching. An important advantage of (N)-CNTs-supported POMs is their fairly good recycling performance. In sharp contrast to POMs immobilized on various active carbons, POM/(N)-CNTs can be easily regenerated after catalytic oxidation and reused without the loss of catalytic activity.

Further research in this area should be aimed at expanding the range of POMs and oxidation reactions (e.g., oxidation of alcohols, oxidative cleavage of C=C bonds, oxyfunctionalization of C-H bonds, and others), as well as studying the mechanisms of POM interaction with the surface of both N-doped CNTs and undoped ones.

Author Contributions: Conceptualization and writing—original draft preparation V.Y.E. and O.A.K.; writing—review and editing O.Y.P. and V.A.L.; investigation, V.A.L.; All authors have read and agreed to the published version of the manuscript.

Funding: This research was funded by the Ministry of Science and Higher Education of the Russian Federation within the governmental order for the Boreskov Institute of Catalysis (project AAAA-A21-121011390008-4).

Acknowledgments: The authors thank all co-authors of the joint papers published on the oxidation catalysis by POM/(N)-CNTs and cited in this article: Arina Suboch (synthesis of (N)-CNTs); Irina Ivanchikova, Nataliya Maksimchuk, and Olga Zalomaeva (catalytic studies); Olga Stonkus (TEM); Lidiya Kibis (XPS); and Yuri Chesalov (FTIR).

Conflicts of Interest: The authors declare no conflict of interest.

References

- Teles, J.H.; Partenheimer, W.; Jira, R.; Cavani, F.; Strukul, G.; Hage, R.; de Boer, J.W.; Goossen, L.; Mamone, P.; Kholdeeva, O.A. Oxidation. In *Applied Homogeneous Catalysis with Organometallic Compounds: A Comprehensive Handbook in Four Volumes*, 3rd ed.; Cornils, B., Hermann, W.A., Beller, M., Paciello, R., Eds.; Wiley-VCH: Weinheim, Germany, 2017; Volume 2, pp. 465–568.
- Duprez, D.; Cavani, F. (Eds.) *Handbook of Advanced Methods and Processes in Oxidation Catalysis*; Imperial College Press: London, UK, 2014.
- Clerici, M.G.; Kholdeeva, O.A. (Eds.) *Liquid Phase Oxidation via Heterogeneous Catalysis: Organic Synthesis and Industrial Applications*; John Wiley & Sons: Hoboken, NJ, USA, 2013.
- Mizuno, N. (Ed.) *Modern Heterogeneous Oxidation Catalysis: Design, Reactions and Characterization*; Wiley-VCH: Weinheim, Germany, 2009.
- Sheldon, R.A. E factors, green chemistry and catalysis: An odyssey. *Chem. Comm.* **2008**, *29*, 3352–3365. [[CrossRef](#)] [[PubMed](#)]
- Campos-Martin, J.M.; Blanco-Brieva, G.; Fierro, J.L. Hydrogen peroxide synthesis: An outlook beyond the anthraquinone process. *Angew. Chem. Int. Ed.* **2006**, *45*, 6962–6984. [[CrossRef](#)] [[PubMed](#)]
- Jones, C.W. *Applications of Hydrogen Peroxide and Derivatives*; Royal Society of Chemistry: Cambridge, UK, 1999.
- Pope, M.T.; Jeannin, Y.; Fournier, M. *Heteropoly and Isopoly Oxometalates*; Springer: Berlin/Heidelberg, Germany, 1983.
- López, X.; Carbó, J.J.; Bo, C.; Poblet, J.M. Structure, properties and reactivity of polyoxometalates: A theoretical perspective. *Chem. Soc. Rev.* **2012**, *41*, 7537–7571. [[CrossRef](#)] [[PubMed](#)]
- Long, D.L.; Tsunashima, R.; Cronin, L. Polyoxometalates: Building blocks for functional nanoscale systems. *Angew. Chem. Int. Ed.* **2010**, *49*, 1736–1758. [[CrossRef](#)]
- Kortz, U.; Mueller, A.; van Slageren, J.; Schnack, J.; Dalal, N.S.; Dressel, M. Polyoxometalates: Fascinating structures, unique magnetic properties. *Coord. Chem. Rev.* **2009**, *253*, 2315–2327. [[CrossRef](#)]
- Hill, C.L.; Prosser-McCartha, C.M. Homogeneous catalysis by transition metal oxygen anion clusters. *Coord. Chem. Rev.* **1995**, *143*, 407–455. [[CrossRef](#)]
- Wang, S.S.; Yang, G.Y. Recent advances in polyoxometalate-catalyzed reactions. *Chem. Rev.* **2015**, *115*, 4893–4962. [[CrossRef](#)]
- Omwoma, S.; Gore, C.T.; Ji, Y.; Hu, C.; Song, Y.F. Environmentally benign polyoxometalate materials. *Coord. Chem. Rev.* **2015**, *286*, 17–29. [[CrossRef](#)]
- Lv, H.; Geletii, Y.V.; Zhao, C.; Vickers, J.W.; Zhu, G.; Luo, Z.; Song, J.; Lian, T.; Musaev, D.G.; Hill, C.L. Polyoxometalate water oxidation catalysts and the production of green fuel. *Chem. Soc. Rev.* **2012**, *41*, 7572–7589. [[CrossRef](#)]
- Hill, C.L. Progress and challenges in polyoxometalate-based catalysis and catalytic materials chemistry. *J. Mol. Cat. A Chem.* **2007**, *262*, 2–6. [[CrossRef](#)]
- Zhou, Y.; Guo, Z.; Hou, W.; Wang, Q.; Wang, J. Polyoxometalate-based phase transfer catalysis for liquid-solid organic reactions: A review. *Cat. Sci. Technol.* **2015**, *5*, 4324–4335. [[CrossRef](#)]
- Ahmadian, M.; Anbia, M. Oxidative desulfurization of liquid fuels using polyoxometalate-based catalysts: A review. *Energy Fuels* **2021**, *35*, 10347–10373. [[CrossRef](#)]
- Vilà-Nadal, L.; Cronin, L. Design and synthesis of polyoxometalate-framework materials from cluster precursors. *Nat. Rev. Mater.* **2017**, *2*, 17054. [[CrossRef](#)]
- Wang, Y.; Weinstock, I.A. Polyoxometalate-decorated nanoparticles. *Chem. Soc. Rev.* **2012**, *41*, 7479–7496. [[CrossRef](#)] [[PubMed](#)]
- Walsh, J.J.; Bond, A.M.; Forster, R.J.; Keyes, T.E. Hybrid polyoxometalate materials for photo (electro-) chemical applications. *Coord. Chem. Rev.* **2016**, *306*, 217–234. [[CrossRef](#)]
- Proust, A.; Matt, B.; Villanneau, R.; Guillemot, G.; Gouzerh, P.; Izzet, G. Functionalization and post-functionalization: A step towards polyoxometalate-based materials. *Chem. Soc. Rev.* **2012**, *41*, 7605–7622. [[CrossRef](#)] [[PubMed](#)]
- Mizuno, N.; Kamata, K. Catalytic oxidation of hydrocarbons with hydrogen peroxide by vanadium-based polyoxometalates. *Coord. Chem. Rev.* **2011**, *255*, 2358–2370. [[CrossRef](#)]
- Mizuno, N.; Yamaguchi, K.; Kamata, K. Epoxidation of olefins with hydrogen peroxide catalyzed by polyoxometalates. *Coord. Chem. Rev.* **2005**, *249*, 1944–1956. [[CrossRef](#)]
- Brégeault, J.M.; Vennat, M.; Salles, L.; Piquemal, J.Y.; Mahha, Y.; Briot, E.; Bakala, P.C.; Atlamsani, A.; Thouvenot, R. From polyoxometalates to polyoxoperoxometalates and back again; potential applications. *J. Mol. Cat. A Chem.* **2006**, *250*, 177–189. [[CrossRef](#)]
- Vazylyev, M.; Sloboda-Rozner, D.; Haimov, A.; Maayan, G.; Neumann, R. Strategies for oxidation catalyzed by polyoxometalates at the interface of homogeneous and heterogeneous catalysis. *Top. Catal.* **2005**, *34*, 93–99. [[CrossRef](#)]
- Neumann, R. Applications of polyoxometalates in homogeneous catalysis. In *Polyoxometalate Molecular Science*; Borrás-Almenar, J.J., Coronado, E., Mueller, A., Pope, M., Eds.; Kluwer Academic Publishers: Dordrecht, The Netherlands, 2003; pp. 327–349.
- Mizuno, N.; Kamata, K.; Yamaguchi, K. Green oxidation reactions by polyoxometalate-based catalysts: From molecular to solid catalysts. *Top. Catal.* **2010**, *53*, 876–893. [[CrossRef](#)]
- Hill, C.L.; Kholdeeva, O.A. Selective liquid phase oxidations in the presence of supported polyoxometalates. In *Liquid Phase Oxidation via Heterogeneous Catalysis: Organic Synthesis and Industrial Applications*; Clerici, M.G., Kholdeeva, O.A., Eds.; John Wiley & Sons: Hoboken, NJ, USA, 2013; pp. 263–319.

30. Samaniyan, M.; Mirzaei, M.; Khajavian, R.; Eshtiagh-Hosseini, H.; Streb, C. Heterogeneous catalysis by polyoxometalates in metal–organic frameworks. *ACS Catal.* **2019**, *9*, 10174–10191. [[CrossRef](#)]
31. Stamate, A.E.; Pavel, O.D.; Zavoianu, R.; Marcu, I.C. Highlights on the catalytic properties of polyoxometalate-intercalated layered double hydroxides: A review. *Catalysts* **2020**, *10*, 57. [[CrossRef](#)]
32. Kholdeeva, O.A.; Maksimchuk, N.V.; Maksimov, G.M. Polyoxometalate-based heterogeneous catalysts for liquid phase selective oxidations: Comparison of different strategies. *Catal. Tod.* **2010**, *157*, 107–113. [[CrossRef](#)]
33. Thompson, D.J.; Zhang, Y.; Ren, T. Polyoxometalate $[\gamma\text{-SiW}_{10}\text{O}_{34}(\text{H}_2\text{O})_2]^{4-}$ on MCM-41 as catalysts for sulfide oxygenation with hydrogen peroxide. *J. Mol. Catal. A Chem.* **2014**, *392*, 188–193. [[CrossRef](#)]
34. Sakamoto, T.; Pac, C. Selective epoxidation of olefins by hydrogen peroxide in water using a polyoxometalate catalyst supported on chemically modified hydrophobic mesoporous silica gel. *Tet. Lett.* **2000**, *41*, 10009–10012. [[CrossRef](#)]
35. Zhao, H.; Zeng, L.; Li, Y.; Liu, C.; Hou, B.; Wu, D.; Feng, N.; Zheng, A.; Xie, X.; Su, S.; et al. Polyoxometalate-based ionic complexes immobilized in mesoporous silicas prepared via a one-pot procedure: Efficient and reusable catalysts for H_2O_2 -mediated alcohol oxidations in aqueous media. *Microporous Mesoporous Mater.* **2013**, *172*, 67–76. [[CrossRef](#)]
36. Mizuno, N.; Yamaguchi, K. Polyoxometalate catalysts: Toward the development of green H_2O_2 -based epoxidation systems. *Chem. Rec.* **2006**, *6*, 12–22. [[CrossRef](#)]
37. Kasai, J.; Nakagawa, Y.; Uchida, S.; Yamaguchi, K.; Mizuno, N. $[\gamma\text{-1,2-H}_2\text{SiV}_2\text{W}_{10}\text{O}_{40}]$ Immobilized on Surface-Modified SiO_2 as a Heterogeneous Catalyst for Liquid-Phase Oxidation with H_2O_2 . *Chem. Eur. J.* **2006**, *12*, 4176–4184. [[CrossRef](#)]
38. Hajian, R.; Jafari, F. Zinc polyoxometalate immobilized on ionic liquid-modified MCM-41: An efficient reusable catalyst for the selective oxidation of alcohols with hydrogen peroxide. *J. Iran. Chem. Soc.* **2019**, *16*, 563–570. [[CrossRef](#)]
39. Yamaguchi, K.; Yoshida, C.; Uchida, S.; Mizuno, N. Peroxotungstate immobilized on ionic liquid-modified silica as a heterogeneous epoxidation catalyst with hydrogen peroxide. *J. Am. Chem. Soc.* **2005**, *127*, 530–531. [[CrossRef](#)] [[PubMed](#)]
40. Craven, M.; Xiao, D.; Kunstmann-Olsen, C.; Kozhevnikova, E.F.; Blanc, F.; Steiner, A.; Kozhevnikov, I.V. Oxidative desulfurization of diesel fuel catalyzed by polyoxometalate immobilized on phosphazene-functionalized silica. *Appl. Catal. B Environ.* **2018**, *231*, 82–91. [[CrossRef](#)]
41. Dong, X.; Wang, D.; Li, K.; Zhen, Y.; Hu, H.; Xue, G. Vanadium-substituted heteropolyacids immobilized on amine-functionalized mesoporous MCM-41: A recyclable catalyst for selective oxidation of alcohols with H_2O_2 . *Mater. Res. Bull.* **2014**, *57*, 210–220. [[CrossRef](#)]
42. Al-Oweini, R.; Aghyarian, S.; El-Rassy, H. Immobilized polyoxometalates onto mesoporous organically-modified silica aerogels as selective heterogeneous catalysts of anthracene oxidation. *J. Sol-Gel Sci. Technol.* **2012**, *61*, 541–550. [[CrossRef](#)]
43. Karimi, Z.; Mahjoub, A.R.; Harati, S.M. Polyoxometalate-based hybrid mesostructured catalysts for green epoxidation of olefins. *Inorg. Chim. Acta* **2011**, *376*, 1–9. [[CrossRef](#)]
44. Kamata, K.; Yonehara, K.; Sumida, Y.; Hirata, K.; Nojima, S.; Mizuno, N. Efficient heterogeneous epoxidation of alkenes by a supported tungsten oxide catalyst. *Angew. Chem. Int. Ed.* **2011**, *50*, 12062–12066. [[CrossRef](#)]
45. Nojima, S.; Kamata, K.; Suzuki, K.; Yamaguchi, K.; Mizuno, N. Selective Oxidation with Aqueous Hydrogen Peroxide by $[\text{PO}_4\{\text{WO}(\text{O}_2)_2\}_4]^{3-}$ Supported on Zinc-Modified Tin Dioxide. *ChemCatChem* **2015**, *7*, 1097–1104. [[CrossRef](#)]
46. Zhang, Z.; Zhang, F.; Zhu, Q.; Zhao, W.; Ma, B.; Ding, Y. Magnetically separable polyoxometalate catalyst for the oxidation of dibenzothiophene with H_2O_2 . *J. Colloid Interface Sci.* **2011**, *360*, 189–194. [[CrossRef](#)]
47. Leng, Y.; Zhao, J.; Jiang, P.; Wang, J. Amphiphilic polyoxometalate-paired polymer coated Fe_3O_4 : Magnetically recyclable catalyst for epoxidation of bio-derived olefins with H_2O_2 . *ACS Appl. Mater. Interfaces* **2014**, *6*, 5947–5954. [[CrossRef](#)]
48. Gholamyan, S.; Khoshnavazi, R.; Rostami, A.; Bahrami, L. Immobilized Sandwich-Type Polyoxometalates $[\text{Mn}_4(\text{XW}_9\text{O}_{34})_2]^{n-}$ on Tb-Doped TiO_2 Nanoparticles as Efficient and Selective Catalysts in the Oxidation of Sulfides and Alcohols. *Catal. Lett.* **2017**, *147*, 71–81. [[CrossRef](#)]
49. Liu, P.; Wang, C.; Li, C. Epoxidation of allylic alcohols on self-assembled polyoxometalates hosted in layered double hydroxides with aqueous H_2O_2 as oxidant. *J. Catal.* **2009**, *262*, 159–168. [[CrossRef](#)]
50. Liu, K.; Yao, Z.; Miras, H.N.; Song, Y.F. Facile immobilization of a Lewis acid polyoxometalate onto layered double hydroxides for highly efficient N-oxidation of pyridine based derivatives and denitrogenation. *ChemCatChem* **2015**, *7*, 3903–3910. [[CrossRef](#)]
51. Mao, H.; Zhu, K.; Lu, X.; Zhang, G.; Yao, C.; Kong, Y.; Liu, J. Restructuring of silica-pillared clay (SPC) through posthydrothermal treatment and application as phosphotungstic acid supports for cyclohexene oxidation. *J. Colloid Interface Sci.* **2015**, *446*, 141–149. [[CrossRef](#)] [[PubMed](#)]
52. Swalus, C.; Farin, B.; Gillard, F.; Devillers, M.; Gaigneaux, E.M. Hybrid peroxotungstophosphate organized catalysts highly active and selective in alkene epoxidation. *Catal. Commun.* **2013**, *37*, 80–84. [[CrossRef](#)]
53. Lang, X.; Li, Z.; Xia, C. $[\alpha\text{-PW}_{12}\text{O}_{40}]^{3-}$ Immobilized on Ionic Liquid-Modified Polymer as a Heterogeneous Catalyst for Alcohol Oxidation with Hydrogen Peroxide. *Synth. Commun.* **2008**, *38*, 1610–1616. [[CrossRef](#)]
54. Maradur, S.P.; Jo, C.; Choi, D.H.; Kim, K.; Ryoo, R. Mesoporous Polymeric Support Retaining High Catalytic Activity of Polyoxotungstate for Liquid-Phase Olefin Epoxidation using H_2O_2 . *ChemCatChem* **2011**, *3*, 1435–1438. [[CrossRef](#)]
55. Peng, C.; Lu, X.H.; Ma, X.T.; Shen, Y.; Wei, C.C.; He, J.; Zhou, D.; Xia, Q.H. Highly efficient epoxidation of cyclohexene with aqueous H_2O_2 over powdered anion-resin supported solid catalysts. *J. Mol. Catal. A Chem.* **2016**, *423*, 393–399. [[CrossRef](#)]
56. Zheng, W.; Wu, M.; Yang, C.; Chen, Y.; Tan, R.; Yin, D. Alcohols selective oxidation with H_2O_2 catalyzed by robust heteropolyanions intercalated in ionic liquid-functionalized graphene oxide. *Mater. Chem. Phys.* **2020**, *256*, 123681. [[CrossRef](#)]

57. Zhang, W.H.; Shen, J.J.; Wu, J.; Liang, X.Y.; Xu, J.; Liu, P.; Xue, B.; Li, Y.X. An amphiphilic graphene oxide-immobilized polyoxometalate-based ionic liquid: A highly efficient triphase transfer catalyst for the selective oxidation of alcohols with aqueous H₂O₂. *Mol. Catal.* **2017**, *443*, 262–269. [[CrossRef](#)]
58. Masteri-Farahani, M.; Alavijeh, M.K.; Hosseini, M.S. Venturolo anion immobilized on the surface of porous activated carbon as heterogeneous catalyst for the epoxidation of olefins. *React. Kinet. Mech. Catal.* **2020**, *130*, 303–315. [[CrossRef](#)]
59. Férey, G.; Mellot-Draznieks, C.; Serre, C.; Millange, F.; Dutour, J.; Surblé, S.; Margiolaki, I. A chromium terephthalate-based solid with unusually large pore volumes and surface area. *Science* **2005**, *309*, 2040–2042. [[CrossRef](#)] [[PubMed](#)]
60. Maksimchuk, N.V.; Timofeeva, M.N.; Melgunov, M.S.; Shmakov, A.N.; Chesalov, Y.A.; Dybtsev, D.N.; Fedin, V.P.; Kholdeeva, O.A. Heterogeneous selective oxidation catalysts based on coordination polymer MIL-101 and transition metal-substituted polyoxometalates. *J. Catal.* **2008**, *257*, 315–323. [[CrossRef](#)]
61. Maksimchuk, N.V.; Kovalenko, K.A.; Arzumanov, S.S.; Chesalov, Y.A.; Melgunov, M.S.; Stepanov, A.G.; Fedin, V.P.; Kholdeeva, O.A. Hybrid polyoxotungstate/MIL-101 materials: Synthesis, characterization, and catalysis of H₂O₂-based alkene epoxidation. *Inorg. Chem.* **2010**, *49*, 2920–2930. [[CrossRef](#)] [[PubMed](#)]
62. Duan, Y.; Wei, W.; Xiao, F.; Xi, Y.; Chen, S.L.; Wang, J.L.; Xu, Y.; Hu, C. High-valent cationic metal-organic macrocycles as novel supports for immobilization and enhancement of activity of polyoxometalate catalysts. *Catal. Sci. Technol.* **2016**, *6*, 8540–8547. [[CrossRef](#)]
63. Zhang, Z.; Zhao, W.; Ma, B.; Ding, Y. The epoxidation of olefins catalyzed by a new heterogeneous polyoxometalate-based catalyst with hydrogen peroxide. *Catal. Comm.* **2010**, *12*, 318–322. [[CrossRef](#)]
64. Nlate, S.; Plaut, L.; Astruc, D. Synthesis of 9- and 27-Armed Tetrakis (diperotungsto)phosphate-Cored Dendrimers and Their Use as Recoverable and Reusable Catalysts in the Oxidation of Alkenes, Sulfides, and Alcohols with Hydrogen Peroxide. *Chem. Eur. J.* **2006**, *12*, 903–914. [[CrossRef](#)] [[PubMed](#)]
65. Chen, G.; Zhou, Y.; Long, Z.; Wang, X.; Li, J.; Wang, J. Mesoporous polyoxometalate-based ionic hybrid as a triphasic catalyst for oxidation of benzyl alcohol with H₂O₂ on water. *ACS Appl. Mater. Interfaces* **2014**, *6*, 4438–4446. [[CrossRef](#)]
66. Qi, W.; Wang, Y.; Li, W.; Wu, L. Surfactant-Encapsulated Polyoxometalates as Immobilized Supramolecular Catalysts for Highly Efficient and Selective Oxidation Reactions. *Chem. Eur. J.* **2010**, *16*, 1068–1078. [[CrossRef](#)]
67. Rezvani, M.A.; Shaterian, M.; Aghmasheh, M. Catalytic oxidative desulphurization of gasoline using amphiphilic polyoxometalate@polymer nanocomposite as an efficient, reusable, and green organic–inorganic hybrid catalyst. *Environ. Technol.* **2020**, *41*, 1219–1231. [[CrossRef](#)]
68. Rezvani, M.A.; Asli, M.A.N.; Oveisi, M.; Babaei, R.; Qasemi, K.; Khandan, S. An organic–inorganic hybrid based on an Anderson-type polyoxometalate immobilized on PVA as a reusable and efficient nanocatalyst for oxidative desulphurization of gasoline. *RSC Adv.* **2016**, *6*, 53069–53079. [[CrossRef](#)]
69. Hua, L.; Chen, J.; Chen, C.; Zhu, W.; Yu, Y.; Zhang, R.; Guo, L.; Song, B.; Gan, H.; Hou, Z. Immobilization of polyoxometalate-based ionic liquid on carboxymethyl cellulose for epoxidation of olefins. *New J. Chem.* **2014**, *38*, 3953–3959. [[CrossRef](#)]
70. Buru, C.T.; Farha, O.K. Strategies for incorporating catalytically active polyoxometalates in metal–organic frameworks for organic transformations. *ACS Appl. Mater. Interfaces* **2020**, *12*, 5345–5360. [[CrossRef](#)] [[PubMed](#)]
71. Niu, Q.; Liu, G.; Lv, Z.; Si, C.; Han, H.; Jin, M. Mono-substituted polyoxometalate clusters@Zr-MOFs: Reactivity, kinetics, and catalysis for cycloolefins-H₂O₂ biphasic reactions. *Mol. Catal.* **2021**, *504*, 111465. [[CrossRef](#)]
72. Song, X.; Hu, D.; Yang, X.; Zhang, H.; Zhang, W.; Li, J.; Jia, M.; Yu, J. Polyoxomolybdic cobalt encapsulated within Zr-based metal-organic frameworks as efficient heterogeneous catalysts for olefins epoxidation. *ACS Sustain. Chem. Eng.* **2019**, *7*, 3624–3631. [[CrossRef](#)]
73. Tangestaninejad, S.; Moghadam, M.; Mirkhani, V.; Mohammadpoor-Baltork, I.; Shams, E.; Salavati, H. Olefin epoxidation with H₂O₂ catalyzed by vanadium-containing polyphosphomolybdates immobilized on TiO₂ nanoparticles under different conditions. *Catal. Comm.* **2008**, *9*, 1001–1009. [[CrossRef](#)]
74. Xiao, Y.; Chen, D.; Ma, N.; Hou, Z.; Hu, M.; Wang, C.; Wang, W. Covalent immobilization of a polyoxometalate in a porous polymer matrix: A heterogeneous catalyst towards sustainability. *RSC Adv.* **2013**, *3*, 21544–21551. [[CrossRef](#)]
75. Guillemot, G.; Matricardi, E.; Chamoreau, L.M.; Thouvenot, R.; Proust, A. Oxidovanadium (V) Anchored to Silanol-Functionalized Polyoxotungstates: Molecular Models for Single-Site Silica-Supported Vanadium Catalysts. *ACS Catal.* **2015**, *5*, 7415–7423. [[CrossRef](#)]
76. Hoegaerts, D.; Sels, B.F.; De Vos, D.E.; Verpoort, F.; Jacobs, P.A. Heterogeneous tungsten-based catalysts for the epoxidation of bulky olefins. *Catal. Tod.* **2000**, *60*, 209–218. [[CrossRef](#)]
77. Zhu, J.; Holmen, A.; Chen, D. Carbon nanomaterials in catalysis: Proton affinity, chemical and electronic properties, and their catalytic consequences. *ChemCatChem* **2013**, *5*, 378–401. [[CrossRef](#)]
78. Toma, F.M.; Sartorel, A.; Iurlo, M.; Carraro, M.; Parisse, P.; Maccato, C.; Rapino, S.; Gonzalez, B.R.; Amenitsch, H.; Da Ros, T.; et al. Efficient water oxidation at carbon nanotube–polyoxometalate electrocatalytic interfaces. *Nat. Chem.* **2010**, *2*, 826–831. [[CrossRef](#)]
79. Jawale, D.V.; Fossard, F.; Miserque, F.; Geertsen, V.; Teillout, A.L.; de Oliveira, P.; Mbomekalle, I.M.; Gravel, E.; Doris, E. Carbon nanotube–polyoxometalate nanohybrids as efficient electro-catalysts for the hydrogen evolution reaction. *Carbon* **2022**, *188*, 523–532. [[CrossRef](#)]
80. Pan, D.; Chen, J.; Tao, W.; Nie, L.; Yao, S. Polyoxometalate-modified carbon nanotubes: New catalyst support for methanol electro-oxidation. *Langmuir* **2006**, *22*, 5872–5876. [[CrossRef](#)] [[PubMed](#)]

81. Ji, Y.; Huang, L.; Hu, J.; Streb, C.; Song, Y.F. Polyoxometalate-functionalized nanocarbon materials for energy conversion, energy storage and sensor systems. *Energy Environ. Sci.* **2015**, *8*, 776–789. [[CrossRef](#)]
82. Iqbal, B.; Jia, X.; Hu, H.; He, L.; Chen, W.; Song, Y.F. Fabrication of redox-active polyoxometalate-based ionic crystals onto single-walled carbon nanotubes as high-performance anode materials for lithium-ion batteries. *Inorg. Chem. Front.* **2020**, *7*, 1420–1427. [[CrossRef](#)]
83. Ji, Y.; Hu, J.; Huang, L.; Chen, W.; Streb, C.; Song, Y.F. Covalent attachment of Anderson-type polyoxometalates to single-walled carbon nanotubes gives enhanced performance electrodes for lithium ion batteries. *Chem. Eur. J.* **2015**, *21*, 6469–6474. [[CrossRef](#)]
84. Chen, W.; Huang, L.; Hu, J.; Li, T.; Jia, F.; Song, Y.F. Connecting carbon nanotubes to polyoxometalate clusters for engineering high-performance anode materials. *Phys. Chem. Chem. Phys.* **2014**, *16*, 19668–19673. [[CrossRef](#)]
85. Kawasaki, N.; Wang, H.; Nakanishi, R.; Hamanaka, S.; Kitaura, R.; Shinohara, H.; Yokoyama, T.; Yoshikawa, H.; Awaga, K. Nanohybridization of polyoxometalate clusters and single-wall carbon nanotubes: Applications in molecular cluster batteries. *Angew. Chem. Int. Ed.* **2011**, *50*, 3471–3474. [[CrossRef](#)]
86. Hu, J.; Ji, Y.; Chen, W.; Streb, C.; Song, Y.F. “Wiring” redox-active polyoxometalates to carbon nanotubes using a sonication-driven periodic functionalization strategy. *Energy Environ. Sci.* **2016**, *9*, 1095–1101. [[CrossRef](#)]
87. Akter, T.; Hu, K.; Lian, K. Investigations of multilayer polyoxometalates-modified carbon nanotubes for electrochemical capacitors. *Electrochim. Acta* **2011**, *56*, 4966–4971. [[CrossRef](#)]
88. Cuentas-Gallegos, A.K.; Martínez-Rosales, R.; Baibarac, M.; Gomez-Romero, P.; Rincón, M.E. Electrochemical supercapacitors based on novel hybrid materials made of carbon nanotubes and polyoxometalates. *Electrochem. Commun.* **2007**, *9*, 2088–2092. [[CrossRef](#)]
89. Ma, D.; Liang, L.; Chen, W.; Liu, H.; Song, Y.F. Covalently Tethered Polyoxometalate-Pyrene Hybrids for Noncovalent Side-wall Functionalization of Single-Walled Carbon Nanotubes as High-Performance Anode Material. *Adv. Funct. Mater.* **2013**, *23*, 6100–6105. [[CrossRef](#)]
90. Hajian, R.; Alghour, Z. Selective oxidation of alcohols with H₂O₂ catalyzed by zinc polyoxometalate immobilized on multi-wall carbon nanotubes modified with ionic liquid. *Chin. Chem. Lett.* **2017**, *28*, 971–975. [[CrossRef](#)]
91. Salavati, H.; Tangestaninejad, S.; Moghadam, M.; Mirkhani, V.; Mohammadpoor-Baltork, I. Sonocatalytic epoxidation of alkenes by vanadium-containing polyphosphomolybdate immobilized on multi-wall carbon nanotubes. *Ultrason. Sonochemistry* **2010**, *17*, 453–459. [[CrossRef](#)] [[PubMed](#)]
92. Wang, R.; Yu, F.; Zhang, G.; Zhao, H. Performance evaluation of the carbon nanotubes supported Cs_{2.5}H_{0.5}PW₁₂O₄₀ as efficient and recoverable catalyst for the oxidative removal of dibenzothiophene. *Catal. Tod.* **2010**, *150*, 37–41. [[CrossRef](#)]
93. Gao, Y.; Gao, R.; Zhang, G.; Zheng, Y.; Zhao, J. Oxidative desulfurization of model fuel in the presence of molecular oxygen over polyoxometalate based catalysts supported on carbon nanotubes. *Fuel* **2018**, *224*, 261–270. [[CrossRef](#)]
94. Giusti, A.; Charron, G.; Mazerat, S.; Compain, J.D.; Mialane, P.; Dolbecq, A.; Riviere, E.; Wernsdorfer, W.; Biboum, R.N.; Keita, B.; et al. Magnetic Bistability of Individual Single-Molecule Magnets Grafted on Single-Wall Carbon Nanotubes. *Angew. Chem. Int. Ed.* **2009**, *48*, 4949–4952. [[CrossRef](#)]
95. Cao, Y.; Mao, S.; Li, M.; Chen, Y.; Wang, Y. Metal/porous carbon composites for heterogeneous catalysis: Old catalysts with improved performance promoted by N-doping. *ACS Catal.* **2017**, *7*, 8090–8112. [[CrossRef](#)]
96. Podyacheva, O.Y.; Ismagilov, Z.R. Nitrogen-doped carbon nanomaterials: To the mechanism of growth, electrical conductivity and application in catalysis. *Catal. Tod.* **2015**, *249*, 12–22. [[CrossRef](#)]
97. Podyacheva, O.Y.; Cherepanova, S.V.; Romanenko, A.I.; Kibis, L.S.; Svintsitskiy, D.A.; Boronin, A.I.; Stonkus, O.A.; Suboch, A.N.; Puzynin, A.V.; Ismagilov, Z.R. Nitrogen doped carbon nanotubes and nanofibers: Composition, structure, electrical conductivity and capacity properties. *Carbon* **2017**, *122*, 475–483. [[CrossRef](#)]
98. Mabena, L.F.; Ray, S.S.; Mhlanga, S.D.; Coville, N.J. Nitrogen-doped carbon nanotubes as a metal catalyst support. *Appl. Nanosci.* **2011**, *1*, 67–77. [[CrossRef](#)]
99. Ayala, P.; Arenal, R.; Rümmele, M.; Rubio, A.; Pichler, T. The doping of carbon nanotubes with nitrogen and their potential applications. *Carbon* **2010**, *48*, 575–586. [[CrossRef](#)]
100. Evtushok, V.Y.; Suboch, A.N.; Podyacheva, O.Y.; Stonkus, O.A.; Zaikovskii, V.I.; Chesalov, Y.A.; Kibis, L.S.; Kholdeeva, O.A. Highly efficient catalysts based on divanadium-substituted polyoxometalate and N-doped carbon nanotubes for selective oxidation of alkylphenols. *ACS Catal.* **2018**, *8*, 1297–1307. [[CrossRef](#)]
101. Evtushok, V.Y.; Ivanchikova, I.D.; Podyacheva, O.Y.; Stonkus, O.A.; Suboch, A.N.; Chesalov, Y.A.; Zalomaeva, O.V.; Kholdeeva, O.A. Carbon nanotubes modified by Venturrello complex as highly efficient catalysts for alkene and thioethers oxidation with hydrogen peroxide. *Front. Chem.* **2019**, *7*, 858. [[CrossRef](#)] [[PubMed](#)]
102. Evtushok, V.Y.; Podyacheva, O.Y.; Suboch, A.N.; Maksimchuk, N.V.; Stonkus, O.A.; Kibis, L.S.; Kholdeeva, O.A. H₂O₂-based selective oxidations by divanadium-substituted polyoxotungstate supported on nitrogen-doped carbon nanomaterials. *Catal. Tod.* **2020**, *354*, 196–203. [[CrossRef](#)]
103. Evtushok, V.Y.; Ivanchikova, I.D.; Lopatkin, V.A.; Maksimchuk, N.V.; Podyacheva, O.Y.; Suboch, A.N.; Stonkus, O.A.; Kholdeeva, O.A. Heterolytic alkene oxidation with H₂O₂ catalyzed by Nb-substituted Lindqvist tungstates immobilized on carbon nanotubes. *Catal. Sci. Technol.* **2021**, *11*, 3198–3207. [[CrossRef](#)]

104. Suboch, A.N.; Cherepanova, S.V.; Kibis, L.S.; Svintsitskiy, A.D.; Stonkus, O.A.; Boronin, A.I.; Chesnokov, V.V.; Romanenko, A.I.; Ismagilov, Z.R.; Podyacheva, O.Y. Aerobic oxidation of syringyl alcohol over N-doped carbon nanotubes. *Fuller. Nanotub. Carbon Nanostructures* **2016**, *24*, 520–530. [[CrossRef](#)]
105. Evtushok, V.Y.; Lopatkin, V.A. unpublished results.
106. Strano, M.S.; Huffman, C.B.; Moore, V.C.; O'Connell, M.J.; Haroz, E.H.; Hubbard, J.; Miller, M.; Rialon, K.; Kitrell, C.; Ramesh, S.; et al. Reversible, band-gap-selective protonation of single-walled carbon nanotubes in solution. *J. Phys. Chem. B* **2003**, *107*, 6979–6985. [[CrossRef](#)]
107. Ramesh, S.; Ericson, L.M.; Davis, V.A.; Saini, R.K.; Kittrell, C.; Pasquali, M.; Billups, W.E.; Adams, W.W.; Hauge, R.H.; Smalley, R.E. Dissolution of pristine single walled carbon nanotubes in superacids by direct protonation. *J. Phys. Chem. B* **2004**, *108*, 8794–8798. [[CrossRef](#)]
108. Parra-Vasquez, A.N.G.; Behabtu, N.; Green, M.J.; Pint, C.L.; Young, C.C.; Schmidt, J.; Kesselman, E.; Goyal, A.; Ajayan, P.M.; Cohen, Y.; et al. Spontaneous dissolution of ultralong single-and multiwalled carbon nanotubes. *ACS Nano* **2010**, *4*, 3969–3978. [[CrossRef](#)]
109. Zalomaeva, O.V.; Podyacheva, O.Y.; Suboch, A.N.; Kibis, L.S.; Kholdeeva, O.A. Aerobic oxidation of syringyl alcohol over N-doped carbon nanotubes. *Appl. Catal. A Gen.* **2022**, *629*, 118424. [[CrossRef](#)]
110. Childs, R.F.; Parrington, B.D. Protonation of Methyl Substituted Phenols in Super Acids. *Can. J. Chem.* **1974**, *52*, 3303–3312. [[CrossRef](#)]
111. Solcà, N.; Dopfer, O. Protonation of aromatic molecules: Competition between ring and oxygen protonation of phenol (Ph) revealed by IR spectra of $\text{PhH}^+ \text{-Ar}_n$. *Chem. Phys. Lett.* **2001**, *342*, 191–199. [[CrossRef](#)]
112. Bulusheva, L.G.; Fedorovskaya, E.O.; Kurennya, A.G.; Okotrub, A.V. Supercapacitor performance of nitrogen-doped carbon nanotube arrays. *Phys. Status Solidi B* **2013**, *250*, 2586–2591. [[CrossRef](#)]
113. Kamata, K.; Sugahara, K.; Ishimoto, R.; Nojima, S.; Okazaki, M.; Matsumoto, T.; Mizuno, N. Highly selective epoxidation of cycloaliphatic alkenes with aqueous hydrogen peroxide catalyzed by $[\text{PO}_4\{\text{WO}(\text{O}_2)_2\}_4]^{3-}$ /Imidazole. *ChemCatChem* **2014**, *6*, 2327–2332. [[CrossRef](#)]
114. Svintsitskiy, D.A.; Kibis, L.S.; Smirnov, D.A.; Suboch, A.N.; Stonkus, O.A.; Podyacheva, O.Y.; Boronin, A.I.; Ismagilov, Z.R. Spectroscopic study of nitrogen distribution in N-doped carbon nanotubes and nanofibers synthesized by catalytic ethylene-ammonia decomposition. *Appl. Surf. Sci.* **2018**, *435*, 1273–1284. [[CrossRef](#)]
115. Sheldon, R.; Kochi, J.K. *Metal-Catalyzed Oxidations of Organic Compounds: Mechanistic Principles and Synthetic Methodology Including Biochemical Processes*; Academic Press: New York, NY, USA, 2012.
116. Zalomaeva, O.V.; Maksimchuk, N.V.; Maksimov, G.M.; Kholdeeva, O.A. Thioether Oxidation with H_2O_2 Catalyzed by Nb-Substituted Polyoxotungstates: Mechanistic Insights. *Eur. J. Inorg. Chem.* **2019**, *2019*, 410–416. [[CrossRef](#)]
117. Maksimchuk, N.V.; Maksimov, G.M.; Evtushok, V.Y.; Ivanchikova, I.D.; Chesalov, Y.A.; Maksimovskaya, R.I.; Kholdeeva, O.A.; Sole-Daura, A.; Poblet, J.M.; Carbo, J.J. Relevance of protons in heterolytic activation of H_2O_2 over Nb (V): Insights from model studies on Nb-substituted polyoxometalates. *ACS Catal.* **2018**, *8*, 9722–9737. [[CrossRef](#)]
118. Duncan, D.C.; Chambers, R.C.; Hecht, E.; Hill, C.L. Mechanism and dynamics in the $\text{H}_3[\text{PW}_{12}\text{O}_{40}]$ -catalyzed selective epoxidation of terminal olefins by H_2O_2 . Formation, reactivity, and stability of $[\text{PO}_4\{\text{WO}(\text{O}_2)_2\}_4]^{3-}$. *J. Am. Chem. Soc.* **1995**, *117*, 681–691. [[CrossRef](#)]
119. Kochkar, H.; Figueras, F. Synthesis of Hydrophobic $\text{TiO}_2\text{-SiO}_2$ Mixed Oxides for the Epoxidation of Cyclohexene. *J. Catal.* **1997**, *171*, 420–430. [[CrossRef](#)]
120. Corma, A.; Esteve, P.; Martinez, A. Solvent effects during the oxidation of olefins and alcohols with hydrogen peroxide on Ti-beta catalyst: The influence of the hydrophilicity–hydrophobicity of the zeolite. *J. Catal.* **1996**, *161*, 11–19. [[CrossRef](#)]
121. Yamazaki, S. An improved methyltrioxorhenium-catalyzed epoxidation of alkenes with hydrogen peroxide. *Org. Biomol. Chem.* **2007**, *5*, 2109–2113. [[CrossRef](#)] [[PubMed](#)]
122. Scott, S.L. A Matter of Life (time) and Death. *ACS Catal.* **2018**, *8*, 8597–8599. [[CrossRef](#)]
123. Kamata, K.; Yonehara, K.; Nakagawa, Y.; Uehara, K.; Mizuno, N. Efficient stereo- and regioselective hydroxylation of alkanes catalysed by a bulky polyoxometalate. *Nat. Chem.* **2010**, *2*, 478–483. [[CrossRef](#)] [[PubMed](#)]
124. Skobelev, I.Y.; Evtushok, V.Y.; Kholdeeva, O.A.; Maksimchuk, N.V.; Maksimovskaya, R.I.; Ricart, J.M.; Poblet, J.M.; Carbó, J.J. Understanding the regioselectivity of aromatic hydroxylation over divanadium-substituted γ -Keggin polyoxotungstate. *ACS Catal.* **2017**, *7*, 8514–8523. [[CrossRef](#)]
125. Ivanchikova, I.D.; Maksimchuk, N.V.; Maksimovskaya, R.I.; Maksimov, G.M.; Kholdeeva, O.A. Highly selective oxidation of alkylphenols to p-benzoquinones with aqueous hydrogen peroxide catalyzed by divanadium-substituted polyoxotungstates. *ACS Catal.* **2014**, *4*, 2706–2713. [[CrossRef](#)]
126. Kamata, K.; Yamaura, T.; Mizuno, N. Chemo- and Regioselective Direct Hydroxylation of Arenes with Hydrogen Peroxide Catalyzed by a Divanadium-Substituted Phosphotungstate. *Angew. Chem. Int. Ed.* **2012**, *51*, 7275–7278. [[CrossRef](#)]